Persistence of learning-induced synapses depends on neurotrophic priming of glucocorticoid receptors

Margarita Arango-Lievano, Amélie Borie, Yann Dromard, Maxime Murat, Michel G Desarménien, Michael J Garabedian, Freddy Jeanneteau

Persistence of learning-induced synapses depends on neurotrophic priming of glucocorticoid receptors

Margarita Arango-Lievano[a], Amelie M. Borie[a], Yann Dromard[a], Maxime Murat[a], Michel G. Desarmenien[a], Michael J. Garabedian[b,1], and Freddy Jeanneteau[a,1]

[a]Department of Neuroscience, Institut de Genomique Fonctionnelle, INSERM, CNRS, University of Montpellier, 34090 Montpellier, France; and [b]Department of Microbiology, New York University Langone Medical Center, New York, NY 10016

Edited by Bruce S. McEwen, The Rockefeller University, New York, NY, and approved May 21, 2019 (received for review February 26, 2019)

Stress can either promote or impair learning and memory. Such opposing effects depend on whether synapses persist or decay after learning. Maintenance of new synapses formed at the time of learning upon neuronal network activation depends on the stress hormone-activated glucocorticoid receptor (GR) and neurotrophic factor release. Whether and how concurrent GR and neurotrophin signaling integrate to modulate synaptic plasticity and learning is not fully understood. Here, we show that deletion of the neurotrophin brain-derived neurotrophic factor (BDNF)–dependent GR-phosphorylation (PO_4) sites impairs long-term memory retention and maintenance of newly formed postsynaptic dendritic spines in the mouse cortex after motor skills training. Chronic stress and the BDNF polymorphism Val66Met disrupt the BDNF-dependent GR-PO_4 pathway necessary for preserving training-induced spines and previously acquired memories. Conversely, enrichment living promotes spine formation but fails to salvage training-related spines in mice lacking BDNF-dependent GR-PO_4 sites, suggesting it is essential for spine consolidation and memory retention. Mechanistically, spine maturation and persistence in the motor cortex depend on synaptic mobilization of the glutamate receptor subunit A1 (GluA1) mediated by GR-PO_4. Together, these findings indicate that regulation of GR-PO_4 via activity-dependent BDNF signaling is important for the formation and maintenance of learning-dependent synapses. They also define a signaling mechanism underlying these effects.

stress | BDNF-Val66Met | two-photon microscopy | learning and memory | LTP

Stress modifies adaptive behaviors such as learning and memory (1). Glucocorticoids are stress hormones that signal via the glucocorticoid receptor (GR) and can either promote or impair learning and memory (2). Whereas prolonged secretion of glucocorticoids during chronic stress disrupts learning and memory, release of glucocorticoids at the time of learning may promote them (3). An acute rise in glucocorticoid levels at the time of learning stimulates the formation and stabilization of new dendritic spines, and eliminates synapses established before learning. New dendritic spines require protein synthesis, which is initiated in the neuronal networks targeted by behavioral experience (4–6). For example, motor learning instructs remodeling of dendritic spines in excitatory neurons of the motor cortex (7–9). Stabilization of new spine synapses forges new learning-induced connectivity that correlates with memory consolidation (10, 11). However, the pathways and molecular mechanisms affecting spine stabilization during learning and memory in vivo are not understood.

Like glucocorticoids via GR, through its receptor TrkB, brain-derived neurotrophic factor (BDNF) stabilizes newly formed synapses and fosters learning and memory (12–14). BDNF is also critical for modulating the impact of stress in the corticolimbic and mesolimbic systems (15, 16). Behavioral actions of glucocorticoids and BDNF are complementary, and play roles in avoidance, fear, coping, and impulse control (17, 18). The influence on GR by the BDNF pathway likely relies on activity-dependent release of BDNF, which is reduced in the BDNF genetic variant Val66Met associated with impaired response to stress (19–21). BDNF signaling through TrkB alters the GR transcriptome through changes in GR-phosphorylation (PO_4) and can affect neuronal plasticity (22–24). However, it remains unclear whether BDNF-dependent GR-PO_4 mediates the persistence of new spines associated with learning and memory, and if activity-dependent secretion of BDNF is also required.

Here, we used two-photon in vivo microscopy of learning-associated dendritic spine remodeling to examine the effects of the BDNF-dependent GR-PO_4 pathway in a newly developed GR-PO_4–deficient mouse and in a mouse carrying the Val66-Met polymorphism of BDNF. We found that GR-PO_4 and BDNF secretion were both important for the formation and maintenance of new spines after learning through the synaptic recruitment of glutamate receptor A1 (GluA1). Our findings uncover an important mechanism for how acute glucocorticoids can direct a cell type-specific response to store and retain new information upon learning. By turning off this mechanism, chronic stress impaired cell type-specific contextual GR response.

Significance

Signal transduction upon activation of receptor tyrosine kinases by neurotrophins and nuclear receptors by glucocorticoids is essential for homeostasis. Phosphorylation (PO_4) is one way these receptors communicate with one another to support homeostatic reactions in learning and memory. Using a newly developed glucocorticoid receptor (GR)-PO_4–deficient knock-in mouse, we show that consolidation of learning-induced neuroplasticity depends on both GR-PO_4 and neurotrophic signaling. Cross-talk between these pathways affects experience-dependent neuroplasticity and behavior, extending previous implications of neurotrophic priming of glucocorticoid response for adaptive plasticity to chronic stress and antidepressant response. Therefore, a disruption of cross-talk between these pathways by, for example, the misalignment of circadian glucocorticoid release and experience-dependent neurotrophic signaling may contribute to the pathophysiology of stress-related disorders.

Author contributions: M.A.-L., A.M.B., M.G.D., and F.J. designed research; M.A.-L., A.M.B., Y.D., M.M., and F.J. performed research; M.A.-L., Y.D., M.J.G., and F.J. contributed new reagents/analytic tools; M.A.-L., A.M.B., Y.D., M.M., and F.J. analyzed data; and M.A.-L., M.J.G., and F.J. wrote the paper.

The authors declare no conflict of interest.

This article is a PNAS Direct Submission.

[1]To whom correspondence may be addressed. Email: michael.garabedian@nyulangone.org or freddy.jeanneteau@igf.cnrs.fr.

This article contains supporting information online at www.pnas.org/lookup/suppl/doi:10.1073/pnas.1903203116/-/DCSupplemental.

Published online June 10, 2019.

Results

Timing and Specificity of BDNF-Dependent GR-PO_4 Expression in Motor Cortex. The corticosterone-GR pathway is required for the acquisition of new motor skills (25), but its dependence on BDNF-dependent GR-PO_4 is unknown. To unravel this, we assessed whether learning might affect GR-PO_4 using a rotarod learning paradigm. Mice were left untrained or trained for 2 d. Forty-five minutes after the training, both control untrained and trained mice were euthanized, and expression in the cortex of GR-PO_4 at the BDNF-dependent sites [S152 and S284 in mice correspond to S155 and S287 in the rat numbering scheme as previously described (23, 26)], as well as c-Fos as an index of neuronal response, was determined by immunohistochemistry. Training increased the level of GR-PO_4 at S152 and S284 in motor areas of cortex compared with the untrained controls (*SI Appendix*, Fig. S1*A*). The Thy1-YFP–marked excitatory and parvalbumin (PV) inhibitory neurons are among the cell types exhibiting high levels of GR-PO_4 in M1 primary motor cortex (*SI Appendix*, Fig. S1*B*). Both cells types displayed increased c-Fos protein abundance upon training. Training also raised the percentage of cells harboring BDNF-dependent GR-PO_4 in all layers of the M1 cortex (*SI Appendix*, Fig. S1*C*). In fact, training also raised the proportion of cells double-labeled with GR-PO_4 and c-Fos (*SI Appendix*, Fig. S1*D*) and increased GR-PO_4 in PV and Thy1 neurons (*SI Appendix*, Fig. S1 *E* and *F*). Induction of GR-PO_4 was site-specific (S152/S284 versus S234; *SI Appendix*, Fig. S1*A*) and did not persist 24 h posttraining, similar to c-Fos in cortical areas relevant for motor skill learning (*SI Appendix*, Fig. S1*G*). Therefore, GR-PO_4 at BDNF-dependent sites increased with training in the motor cortex and is linked to neuronal c-Fos response.

Deletion of GR-PO_4 at BDNF-Responding Sites Impaired Motor Skill Retention. We next determined whether GR-PO_4 at the BDNF-dependent sites affected learning and memory, as well as plasticity of dendritic spines. To do this, we generated a conditional allele of GR consisting of exon 2 harboring serine-to-alanine mutations in the BDNF-dependent GR-PO_4 sites S152A and S284A [sites S134 and S267 in human GR and sites S155 and S287 in the rat GR numbering scheme (Fig. 1*A*)]. Recombination into germ cells using the constitutive ROSA26-CRE mouse line resulted in the mutations being stably transmitted to next generations (*SI Appendix*, Fig. S3). Cortical tissue from the GR-PO_4–deficient knock-in (KI) mouse showed no staining with GR-PO_4–specific antibodies compared with littermate wild-type (WT) controls (Fig. 1*B*). The same protein abundance of total GR was observed between the WT and KI mice (*SI Appendix*, Fig. S4). Likewise, mineralocorticoid receptor levels were unaffected in KI mice (*SI Appendix*, Fig. S4). Therefore, the KI mutant mice eliminated GR-PO_4 without affecting the abundance of GRs.

Deletion of the BDNF-dependent GR-PO_4 sites resulted in adult mice of normal appearance and body weight under standard, stressed, or enriched living conditions. There was no significant difference between the KI and WT mice in their degree of anxiety (as measured by thigmotaxis and an elevated maze test) (*SI Appendix*, Fig. S5 *A* and *B*), despair behaviors (as assessed by tail suspension and a forced swim test) (*SI Appendix*, Fig. S5 *C* and *D*), and locomotor activity when reared in standard living conditions, as well as in stressful or enriched environmental conditions (Fig. 1*C*), previously shown to activate the corticosterone-GR pathway (27). KI mice exhibited normal learning abilities of new motor skills on the rotarod but impaired retention of the task compared with WT littermates (Fig. 1*D*). Retention of new rotarod motor skills was also impaired in WT mice if exposed to chronic unpredictable stress immediately after training during the consolidation period, whereas enrichment living had no impact (Fig. 1*E*). This is consistent with the reduction of BDNF-dependent GR-PO_4 in motor cortex of mice reared in chronic stress conditions (Fig. 1*F*). What is more, training-induced c-Fos expression in the excitatory and inhibitory (PV) neurons was reduced in KI mice compared with WT controls (Fig. 1 *H* and *I*). The effect of the KI showed in specific layers of the cortex differently whether in PV or neurogranin (NG) cells, suggesting putative interlayer network compensation in KI mice. Therefore, GR-PO_4 disruption impaired activation of M1 cortex, as determined by c-Fos expression, as well as motor skill retention, which both depend on BDNF and corticosterone (25, 28).

GR-PO_4 Is Required for the Maintenance of New Dendritic Spines Formed at Training. Previous studies have shown that de novo spine formation and maintenance contribute to the storage of new motor skills by creating new synaptic connections in the M1 region of the motor cortex (29). Therefore, we assessed how learning-associated spine formation in deep layer excitatory neurons (Thy1-YFP) varied with GR-PO_4, using transcranial two-photon microscopy (Fig. 2*A*). As expected, the majority of spines were stable, such that only a small subset of spines was dynamic after training (Fig. 2*B*). Rates of spine formation (Fig. 2*C*) and elimination (Fig. 2*D*) were undistinguishable between WT and KI mice when untrained. However, after training, KI mice exhibited reduced spine formation (Fig. 2*C*) and excessive spine elimination (Fig. 2*D*) that corresponded to a net decrease of total spine number compared with WT littermates (Fig. 2*E*). Spine maintenance was also diminished in KI mice. This included both training-induced new spines and preexisting old spines present before training (Fig. 2*F*). In fact, the more training-induced new spines that survived the consolidation period, the better was the retention of motor skill performance (Fig. 2*G*).

To ensure that the BDNF-dependent GR-PO_4 effect on experience-dependent spine plasticity was cell-autonomous in excitatory neurons of M1 cortex, we exclusively targeted this set of neurons by in utero electroporation (*SI Appendix*, Fig. S6 *A*–*C*). Substitution of endogenous GR with the PO_4-deficient GR mutant as previously described (30) decreased spine formation and increased spine elimination in layer 1 of M1 cortex after training, which is consistent with a net decrease of spine density observed in the KI mice. This indicates that the effect of GR-PO_4 is cell-autonomous.

Chronic unpredictable stress in WT mice decreased spine formation, increased spine elimination (*SI Appendix*, Fig. S6 *D* and *E*) during training, and reduced spine survival during the consolidation period, thus mimicking the effect of KI on spine dynamics, motor skills learning, and memory. KI mice showed net spine loss exaggerated with training and no further impact of chronic unpredictable stress on spine formation, elimination, and consolidation (Fig. 2*F* and *SI Appendix*, Fig. S6*F*). The lack of any additive effects between chronic stress and deletion of the GR-PO_4 sites on spine plasticity indicates a functional redundancy of these pathways. This contrasts with the lack of effects of enrichment living on spine elimination, survival, and motor performance (Fig. 2 *F* and *G*). Remarkably, enrichment living reversed spine formation defects in KI mice (*SI Appendix*, Fig. S6 *D* and *E*). However, this did not enhance motor retention, because the new spines were unrelated to the training. This is in agreement with a role of BDNF-dependent GR-PO_4 on the maintenance of training-dependent new spines for better retention of motor performance (Fig. 2*G*).

BDNF-Val66Met Polymorphism Recapitulated Synaptic and Motor Defects of GR-PO_4 Deletion. The BDNF-Val66Met polymorphism impairs activity-dependent secretion of BDNF and manifests as defective motor skill training in rodents and humans (28, 31). This phenotype is similar to that observed in the KI mice. Therefore, we tested functional epistasis between KI and BDNF-Val66Met to

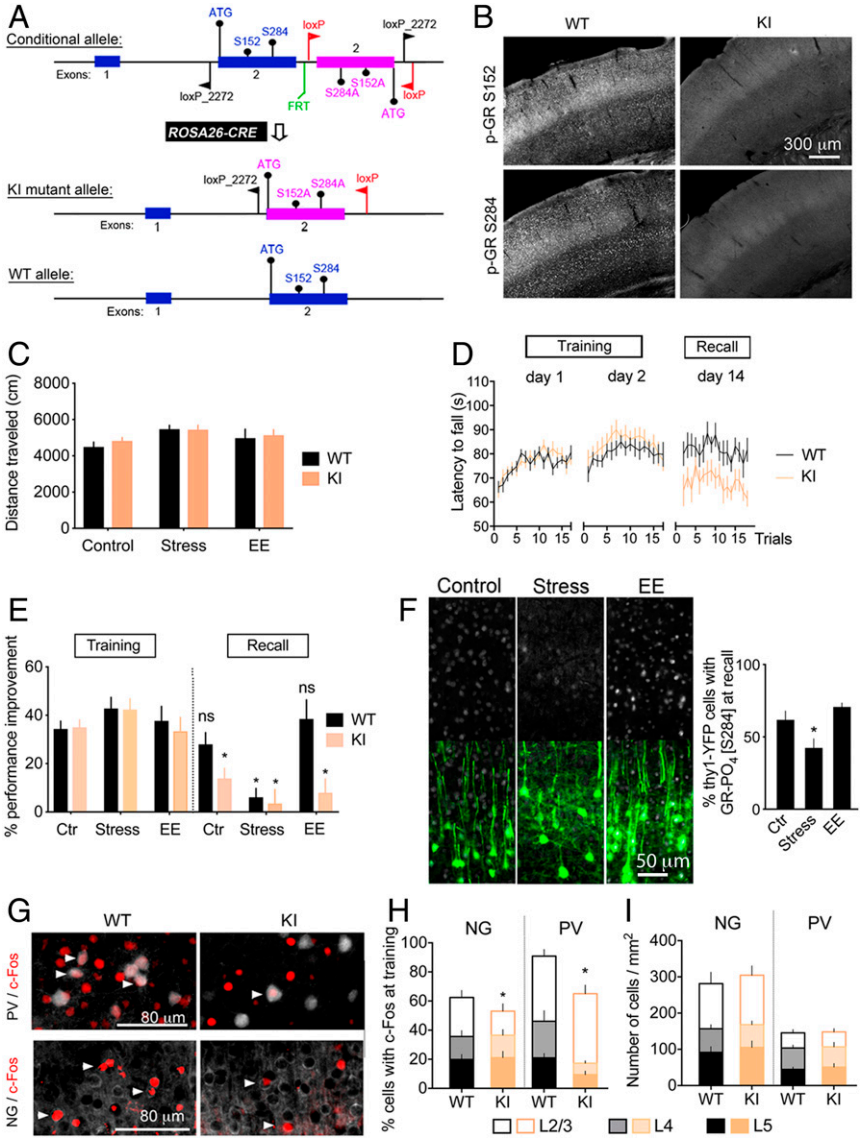

Fig. 1. Deletion of BDNF-dependent GR-PO_4 impairs retention of motor skill training. (*A*) Substitution of Ser152 and Ser284 (WT allele) by Ala152 and Ala284 (KI allele) in GR locus obtained by Cre-mediated recombination of loxP sites driven by the Rosa26 promoter. KI mice lack BDNF-dependent GR-PO_4 sites. Details of the genetic constructs can be found in *Methods* and *SI Appendix*, Fig. S2. (*B*) Deletion of GR-PO_4 immunostaining in KI homozygous mice compared with WT controls. (*C*) Spontaneous locomotion in an open field of mice reared in a control condition, chronic stress condition, or enriched environment (EE) for 2 wk starting immediately after the training. Mean ± SEM of $n = 8$ mice per group; two-way ANOVA: general effect of living conditions ($F_{2,42} = 3.43$, $P = 0.039$). (*D*) Motor skill learning monitored after 2 wk of consolidation displayed as the latency to fall from the rotarod. Mean ± SEM of $n = 8$ mice per group; three-way ANOVA: effect of genotype ($F_{2,2} = 3.075$, $P < 0.05$), post hoc Tukey test: WT day 2 ($P = 0.035$), KI day 2 ($P = 0.017$); effect on retention ($F_{1,2} = 11.33$, $P < 0.05$), post hoc Tukey test: KI ($P = 0.015$). (*E*) Rotarod performance improvement to day 1 of mice reared in control, stress, or EE conditions for 2 wk after the training. Mean ± SEM of $n = 8$ mice per group; three-way ANOVA: effect of retention ($F_{1,84} = 52.17$, $P < 0.0001$), genotype ($F_{1,84} = 9.1$, $P < 0.01$), stress × retention ($F_{2,84} = 7.8$, $P < 0.001$), and genotype × retention ($F_{2,84} = 6.55$, $P < 0.05$); post hoc Tukey test between training and recall (*$P < 0.05$). ns, not significant. (*F*) Effect of stress and EE between days 3 and 14 on GR-PO_4 levels (gray) in Thy1-YFP neurons (green) of M1 cortex. Mean ± SEM of $n = 8$ mice per group; unpaired *t* test [$t_{(14)} = 2.21$, *$P < 0.05$]. Larger fields of view are shown in *SI Appendix*, Fig. S2. (*G*) Expression of c-Fos 45 min after 2 d of training in L2/3 NG principal cells and L5 PV neurons of M1. Arrowheads point to coexpression. Magnified photographs are shown in *SI Appendix*, Fig. S2. (*H*) Mean ± SEM of $n = 5$ mice per group; three-way ANOVA: effect of genotype: ($F_{1,48} = 8.33$, $P = 0.0058$), effect of cell type ($F_{1,48} = 10.95$, $P = 0.0018$), and effect in cortical layers ($F_{2,48} = 31.24$, $P < 0.0001$); post hoc Tukey test for NG cells L2/3 (*$P = 0.026$), L4 ($P = 0.93$), and L5 ($P = 0.77$); post hoc Tukey test for PV cells L2/3 ($P = 0.58$), L4 (*$P = 0.004$), and L5 (*$P = 0.046$). (*I*) Number of NG and PV neurons per square millimeter in M1. Mean ± SEM of $n = 5$ mice per group.

determine whether both pathways converge during motor skills learning. We found that BDNF-dependent GR-PO_4 was reduced in mouse carriers of the BDNF-Val66Met allele (Fig. 3*A*). We then crossed heterozygous KI;Thy1-YFP mice with heterozygous BDNF-Val66Met;Thy1-YFP mice to obtain homozygotes. Four groups of mice, WT, KI, M (BDNF-Val66Met), and M;KI (KI::BDNF-Val66Met), were subjected to in vivo imaging of dendritic spines upon motor skill training. M mice exhibited normal acquisition but impaired retention of the motor task. Importantly, the M;KI double-mutant mice showed no additional effect (Fig. 3*B*). As expected, spine plasticity in the M mice was defective during training but was unaffected in the untrained groups (Fig. 3*C*). Defects in spine elimination and spine survival in the M mice recapitulated those of the KI mice, with no additive effects in the M;KI double-mutants (Fig. 3 *C* and *D*). Together, these results indicated that KI mice and M mice (with impaired activity-dependent

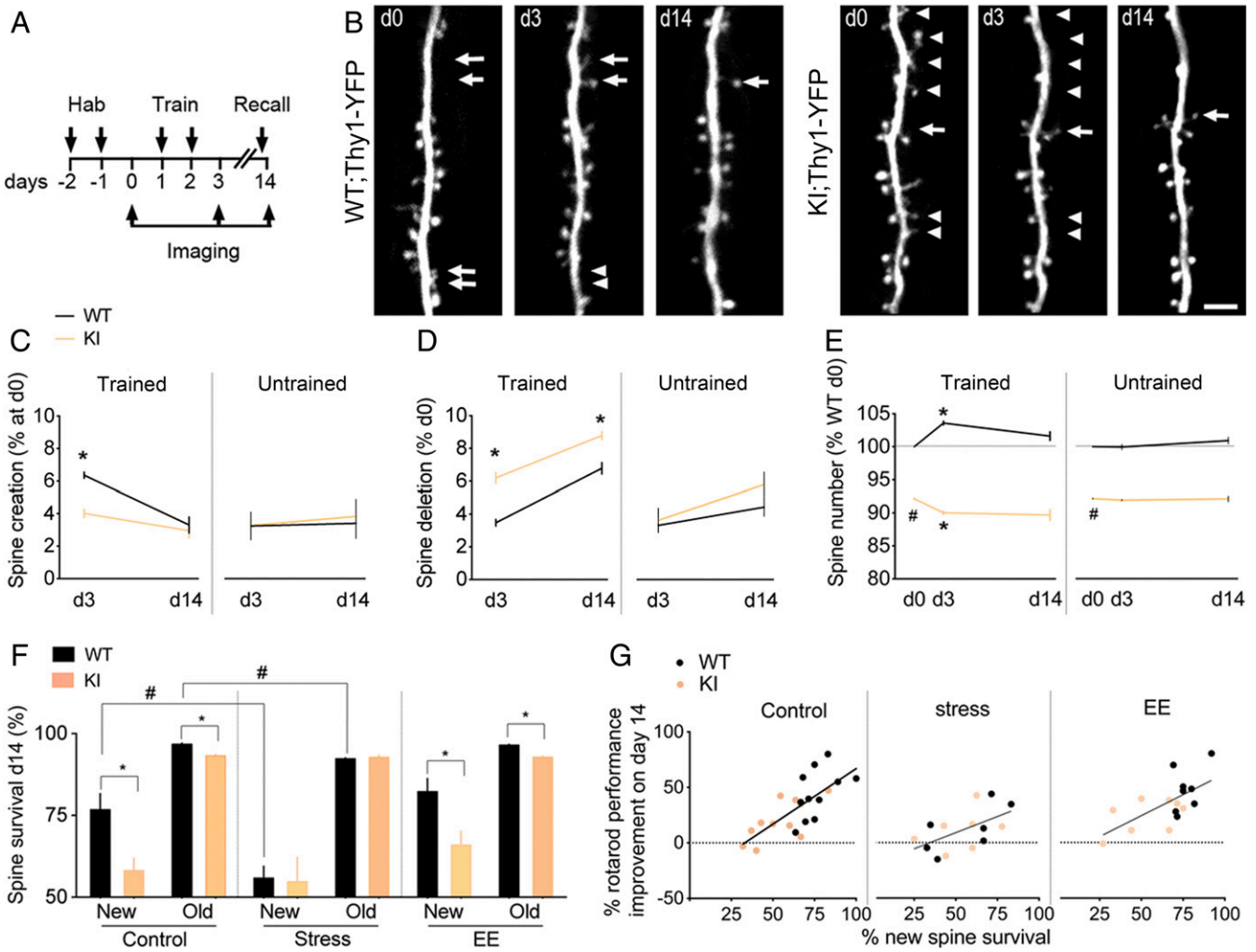

Fig. 2. GR-PO_4 is required for the maintenance of new spines formed at training. (*A*) Timeline of dendritic spine imaging in M1 cortex of GR-KI;Thy1-YFP mice habituated to the nonaccelerating rod (2 rpm) for 2 d before training at the circadian peak of corticosterone (7:00 PM) on the accelerating rod (up to 80 rpm). A recall session on the accelerating rod is performed before the last imaging session on day 14. (*B*) Dendritic spine dynamics of L5 principal Thy1-YFP neurons in L1 of M1 as a function of genotype and time. Arrows point to spine creations, and arrowheads point to spine deletions (Scale bar, 5 μm). d, day. (*C*) Spine creation in M1. Mean ± SEM of $n = 20$ trained WT mice on days 0–3 and 6 on day 14, $n = 18$ trained KI mice on days 0–3 and 7 on day 14, $n = 6$ untrained WT mice on days 0–14, and $n = 7$ untrained KI mice on days 0–14; three-way ANOVA: effect of genotype × training ($F_{1,69} = 4.39$, $P < 0.05$), post hoc Tukey test: WT vs. KI ($^{*}P < 0.0005$). d, day. (*D*) Spine deletion in M1. Mean ± SEM of $n = 20$ trained WT mice on days 0–3 and 6 on day 14; $n = 18$ trained KI mice on days 0–3 and 7 on day 14, $n = 6$ untrained WT mice on days 0–14, and $n = 7$ untrained KI mice on days 0–14; three-way ANOVA: effect of genotype ($F_{1,69} = 23.28$, $P < 0.0001$) and genotype × training ($F_{1,69} = 5.3$, $P < 0.05$), post hoc Tukey test: WT vs. KI ($^{*}P < 0.05$). (*E*) Spine number in M1 relative to WT control. Mean ± SEM of $n = 20$ trained WT mice on days 0–3 and 6 on day 14, $n = 18$ trained KI mice on days 0–3 and 7 on day 14, $n = 6$ untrained WT mice on days 0–14, and $n = 7$ untrained KI mice on days 0–14; three-way ANOVA: effect of genotype ($F_{1,116} = 2453$, $P < 0.0001$) and genotype × training ($F_{1,116} = 55.18$, $P < 0.0001$), post hoc Tukey test: WT vs. KI ($^{\#}P < 0.0001$) and day 0 vs. day 3 ($^{*}P < 0.0001$). (*F*) Survival of training-induced new spines and preexisting old spines in M1. Mean ± SEM of $n = 11$ control mice per group, 7 stress mice per group; 8 enriched environment (EE) mice per group; three-way ANOVA: effect of stress ($F_{1,64} = 8.1$, $P = 0.059$), post hoc Tukey test: WT ($^{\#}P < 0.005$). Pairwise comparisons by unpaired *t* test for the effect of genotype on control new spines [$t_{(20)} = 2.99$, $^{*}P = 0.007$] and control old spines [$t_{(20)} = 6.9$, $^{*}P < 0.0001$] and on new spines EE [$t_{(14)} = 2.78$, $^{*}P = 0.014$] and old spines [EE $t_{(14)} = 7.93$, $^{*}P < 0.0001$]. Spine addition and elimination data are shown in *SI Appendix*, Fig. S6. (*G*) Correlation between survival at day 14 of spines that formed during training on day 2 and memory retention on day 14 in control conditions (Pearson $r = 0.73$, $P = 0.0001$, $n = 11$ WT, $n = 11$ KI), chronic stress ($r = 0.56$, $P = 0.036$, $n = 7$ WT, $n = 7$ KI), or EE ($r = 0.64$, $P = 0.0006$, $n = 8$ WT, $n = 8$ KI).

BDNF secretion) have a reduction in their ability to stabilize the new training-induced spines and retain new motor skills. This is consistent with the convergence of both pathways toward new spine consolidation.

Poorer Retention Was Consistent with Weaker Long-Term Potentiation in Motor Cortex upon GR-PO_4 Deletion. Potentiation of excitatory synaptic transmission in the M1 motor cortex is required to acquire and retain new motor skills (32). To test whether KI mice showed defects in synaptic plasticity, we performed tetanus-induced long-term potentiation (LTP) 1 d posttraining. LTP can be induced in WT and KI mice, regardless of training (Fig. 4 *A* and *B*). After three consecutive tetanus stimulations, LTP saturated in the trained cortex of WT but not KI mice (Fig. 4 *B* and *C*). These data suggested that training occluded LTP in WT but not KI mice (Fig. 4*D*). In fact, LTP occlusion after serial inductions can predict retention of motor skills learning in rodents and humans (33–35). In the KI mice, we find that LTP occlusion was weaker and retention was poorer compared with WT littermates (Fig. 4*E*). This indicates that GR-PO_4 is essential for functional strengthening of M1 synapses posttraining.

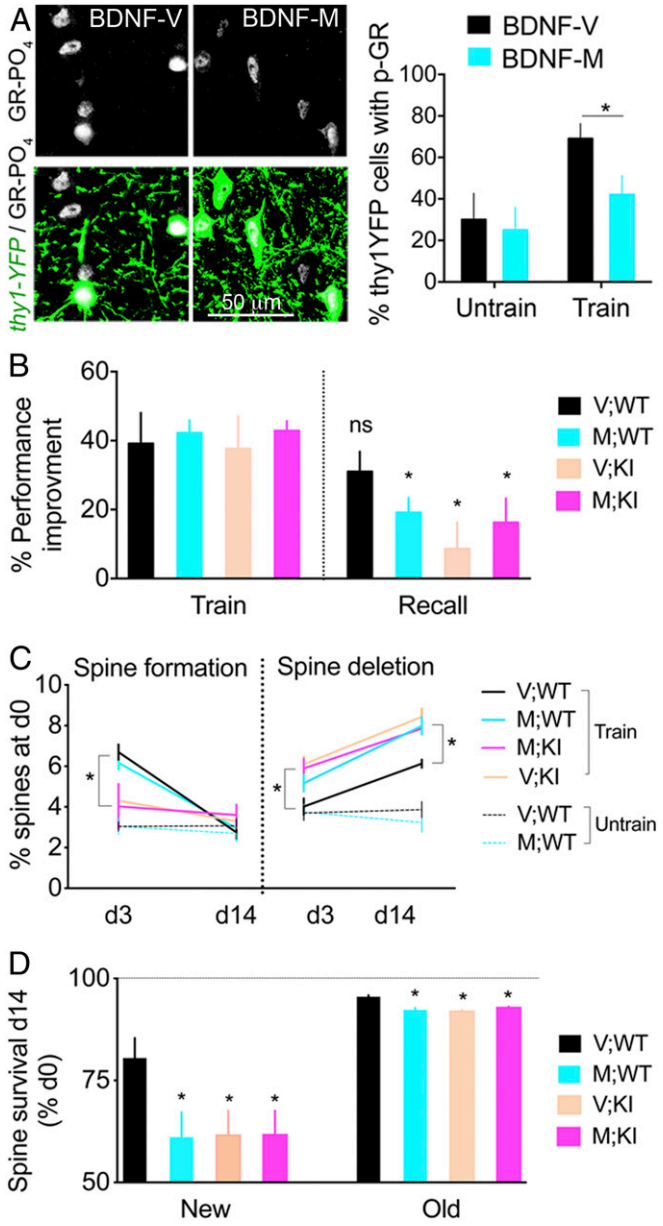

Fig. 3. BDNF-dependent GR-PO_4 is required for training-evoked spine survival and motor skill retention. (*A*) Effect of BDNF-Val66Met polymorphism on GR-PO_4 staining in Thy1-YFP neurons of M1 cortex after 2 d of rotarod training. Mean ± SEM of $n = 5$ untrained mice per group, 7V (BDNF-Val/Val), and 8M (BDNF-Met/Met) trained; two-way ANOVA ($F_{1,21} = 7.75$, $P = 0.011$). Pairwise group comparison between BDNF-M and BDNF-V by unpaired t test [$t_{(13)} = 2.24$, $^*P < 0.05$]. (*B*) Effect of genotypes on rotarod performance at recall on day 14 expressed as a percentage of day 1 in GR-KI mice backcrossed with the BDNF-Val66Met background. Mean ± SEM of $n = 8$ V;WT mice, 8 M;WT mice, 9 V;KI mice, and 11 M;KI mice; three-way ANOVA: effect on retention ($F_{1,64} = 23.68$, $P < 0.0001$), post hoc Tukey test ($^*P < 0.05$). ns, not significant. (*C*) Spine formation in M1. Mean ± SEM of $n = 7$ V;WT trained mice, $n = 7$ M;WT trained mice, $n = 7$ V;KI trained mice, $n = 8$ M;KI trained mice, $n = 8$ V;WT untrained mice, and $n = 5$ M;WT untrained mice; two-way ANOVA: effect of genotype ($F_{3,50} = 4.65$) and time ($F_{1,50} = 91.55$, $P < 0.01$), post hoc Tukey test ($^*P < 0.0001$). Spine deletion. Effect of genotype ($F_{3,50} = 12.66$) and time ($F_{1,50} = 73.12$, $P < 0.0001$), post hoc Tukey test ($^*P < 0.05$). d, day. (*D*) Survival of new spines in M1 formed on day 3 and old spines formed before day 0. Mean ± SEM of $n = 7$ V;WT mice, $n = 8$ M;WT mice, $n = 9$ V;KI mice, and $n = 11$ M;KI mice; two-way ANOVA: effect of genotype ($F_{3,62} = 2.88$, $P < 0.05$). Pairwise comparisons by unpaired t test between V;WT mice and M;WT mice on new spines [$t_{(13)} = 2.28$] and old spines [$t_{(13)} = 4.86$]; V;WT mice and V;KI mice on new spines [$t_{(14)} = 2.24$] and old spines [$t_{(14)} = 9.95$]; and V;WT mice and M;KI mice on new spines [$t_{(16)} = 2.15$] and old spines [$t_{(16)} = 7.91$, $^*P < 0.05$].

GR-PO_4 Is Required for Synaptic Mobilization of Phosphorylated GluA1. Synaptic delivery of α-amino-3-hydroxy-5-methyl-4-isoxazolepropionic acid (AMPA)–type glutamate receptors is thought to contribute to LTP (36). In motor cortex, skill training drives AMPA-type GluA1 to postsynapses, contributing to the dynamic changes of glutamatergic synaptic strength (32). Therefore, we tested whether GR-PO_4 and training have an impact on GluA1 synaptic content and PO_4 because these regulate AMPA conductance and synaptic strength (37, 38). We first determined if there was a difference in levels of synaptic GluA1 between trained and untrained groups. Synaptosomes were isolated from M1 cortex collected 45 min after training, and synaptic GluA1 levels were determined using Western blot analysis (*SI Appendix*, Fig. S7). Levels of GluA1 were similar in all groups. However, the level of GluA1 PO_4 at S831 increased as a function of training in WT but not KI mice. As GluA1 PO_4 at this site has been linked to synaptic potentiation in M1 (39), its lack of increase posttraining could reflect LTP defects observed in KI mice posttraining.

We next investigated cell surface delivery of GluA1 using an established biotinylation assay in cultured cortical neurons (40) (*SI Appendix*, Fig. S8*A*). Avidin pulldown of biotin-tagged GluA1 newly inserted at the cell surface was detected by Western blot analysis (Fig. 5*A*). Upon costimulation of the BDNF and GR pathways, levels of GluA1 and its PO_4 isoform were lower in neurons expressing GR-KI mutant compared with GR-WT (Fig. 5*B*). This effect was specific for GluA1 (*SI Appendix*, Fig. S8*B*). These results suggest that GR-PO_4 at the time of training promotes the mobilization of synaptic GluA1. Does this permit the structural maturation and stabilization of training-dependent spines?

GR-PO_4 Pathway Is Required for Strengthening Glutamatergic Response Posttraining. Training-induced LTP occlusion has been previously associated with enlargement of dendritic spine heads in upper layers of motor cortex, a process dependent on glutamate (41). Therefore, we tested the role of GR-PO_4 on glutamate-dependent structural maturation of dendritic spines in vivo. To this end, we used time-lapse imaging of dendritic spines and two-photon uncaging of 4-methoxy-7-nitroindolinyl–caged L-glutamate (MNI-glutamate) directly into M1 cortex through a cranial window (Fig. 5*C*). Glutamate uncaging on the spine head causes its enlargement without affecting unstimulated neighboring spines (Fig. 5*D*). Photostimulation of spines in the absence of MNI-glutamate had no effect, confirming the specificity of the glutamate uncaging response. In trained mice, the rate of glutamate-evoked spine enlargement was 79 ± 11% in WT mice and 59 ± 8% in KI mice. Glutamate-evoked spine enlargement is also slower in KI mice than in WT mice (Fig. 5*E*). Thus, glutamate-induced spine maturation is weaker in KI mice than in WT mice.

Pharmacological blockade of GR with RU486 administered immediately before training impaired the glutamate response of dendritic spines in WT controls, whereas no further inhibition of the response was observed in KI mice (Fig. 5*F*). The lack of additive effects between the deletion of GR-PO_4 and GR inhibition indicated functional redundancy. In contrast, RU486 administered after training had no effect on the glutamate response of dendritic spines (*SI Appendix*, Fig. S9). This further indicates that BDNF-dependent GR-PO_4 at training is required for the strengthening of the glutamatergic response of dendritic spines after training.

Discussion

Using a newly developed GR-PO_4 site-deficient KI mouse, we have expanded on our previous report (23) describing the impact

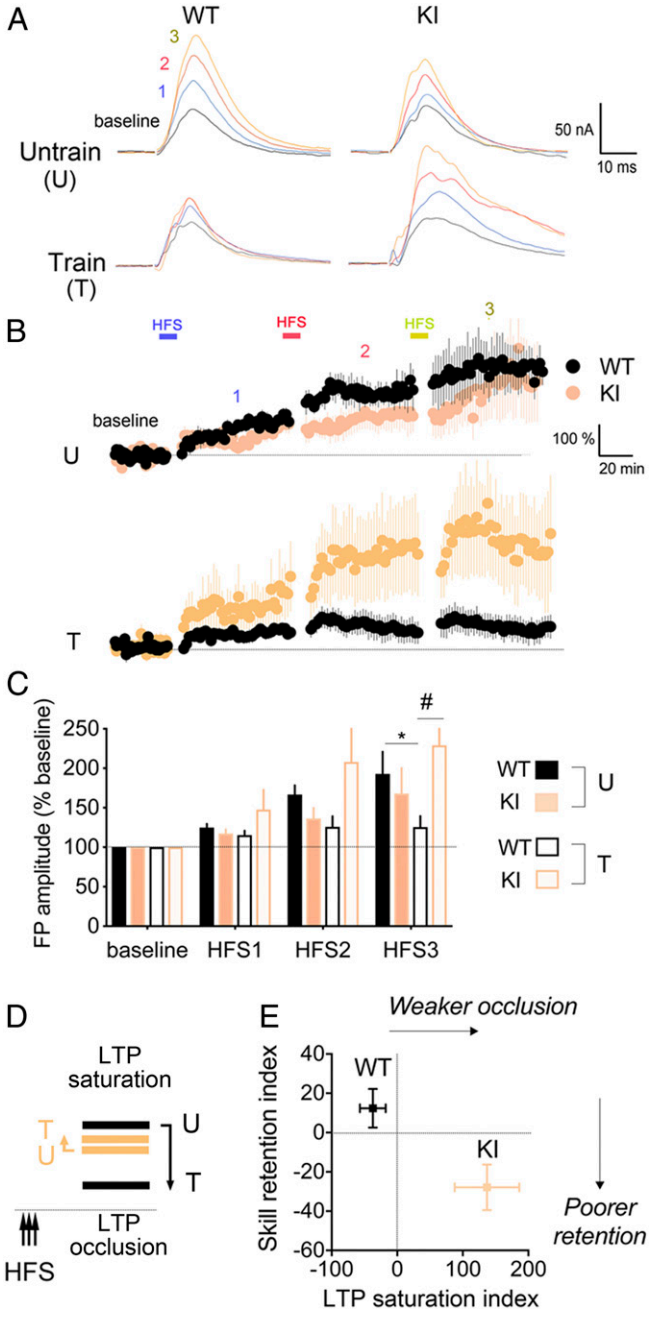

Fig. 4. GR-PO_4 is required for training-evoked plasticity in motor cortex. (*A*) Field potential recordings of high-frequency stimulation (HFS)–induced LTP in M1 cortical slices as a function of genotype and training for 2 d on the rotarod. Acute slices on the next day of training are stimulated with half the intensity to reach a maximal response in L2 parallel fibers at a distance ≈500 μm from the recording electrodes in L2 of M1 cortex. There is a 20-min baseline recording between HFSs. (*B*) FP recordings of tetanus-induced LTP in M1 cortical slices from eight WT and five KI trained mice and five WT and six KI untrained mice. Means are normalized to baseline ± SEM. (*C*) Averaged field potential (FP) amplitudes after three consecutive HFSs (mean of last 40 min per epoch ± SEM). LTP occlusion after HFS3 by unpaired *t* test in WT mice (*$P = 0.034$). Three-way ANOVA: effect of HFS ($F_{3,80} = 13.16$, $P < 0.0001$), genotype ($F_{1,80} = 4.57$, $P < 0.05$), and genotype × training ($F_{1,80} = 14.18$, $P < 0.005$); post hoc Tukey test ($^{\#}P = 0.011$). (*D*) Working model. Training in WT but not KI mice occluded LTP saturation. The dashed line represents baseline transmission in M1. (*E*) Weaker LTP occlusion in KI mice corresponded to poorer retention of motor skills. Motor skill retention and LTP saturation indexes are described in *Methods*. Effect of genotype on LTP occlusion by unpaired *t* test ($P = 0.0055$) (mean ± SEM [$t_{(14)} = 3.28$], $n = 8$ mice per group) and on motor skill retention ($P = 0.014$) (mean ± SEM [$t_{(22)} = 2.64$], $n = 12$ mice per group).

of BDNF-dependent GR-PO_4 on neuronal plasticity and demonstrated the requirement for BDNF activity-dependent release in remodeling of excitatory synapses in the cortex upon learning, as well as its impact on behavior. Our study reveals that either the lack of GR-PO_4 induced by mutation of the BDNF-dependent PO_4 sites or decreased activity-dependent BDNF secretion modeled in the BDNF-Val66Met mutant reduced the survival of learning-associated new spines and impaired memory retention. Moreover, combining the BDNF-Val66Met with the GR-PO_4 mutant mice does not induce further deficits on spine maintenance and behavior as in the individual mutants, indicating that the effect of GR-PO_4 on spine dynamics occurs via BDNF. In agreement with this finding is an increase in GR-PO_4 in the motor cortex by motor skills training, as well as reduced sensitivity to corticosterone and stress in humans and mice with the BDNF-Val66Met allele (20, 42). The physiological role of GR-PO_4 is revealed when the BDNF and GR signaling pathways are paired (26). Permissive actions of BDNF on GR physiological responses can be explained because GR-PO_4 comes about by the activation of kinases through the BDNF-TrkB pathway and the deactivation of phosphatases by the GR-HSP90 pathway (23). Mice lacking GR-PO_4 sites will be instrumental in unraveling the physiological consequences of BDNF and glucocorticoid secretion alignment (e.g., circadian variations, novelty, learning, stress-related diseases, antidepressant treatment) (18, 43). Timing of BDNF and glucocorticoid secretion is brain region-specific, cued to behavioral experience, and could change the neuroplasticity of cells equipped with both GR and TrkB receptors. This is the case in PV and pyramidal cortical neurons, which express high GR-PO_4 levels and in which interconnectivity modulates the dendritic spine elimination response to circadian learning, stress, and antidepressant treatment (25, 44, 45).

Our findings also shed light on the molecular mechanisms underlying how information in the brain is stored (i.e., motor engram) in response to external stimuli, including stress and enriched environment. We observed that chronic stress increased the turnover of spines in WT mice but not in the GR-PO_4 deletion mice as both stress and GR-PO_4 deletion resulted a net loss of training-induced new spines in the cortex. This highlights the critical role of BDNF-dependent GR-PO_4 on the maintenance and connectivity of new training-induced spines within a motor engram. Our findings also predict that physical exercise and/or an enriched environment would promote spine maintenance in cortex, by transforming the training-related new spines into a persistent pool of memory spines, and alleviate the impact of stress on the synaptic engram (45, 46). Motor learning was also associated with an increase in the active phosphorylated form of the GluA1 into synapses that stabilize and strengthen training-related newly formed spines and motor skill retention (37, 47). These effects were reduced in GR-PO_4 deletion mice and recapitulated by GR inhibition with RU486 or chronic stress, which diminished GR-PO_4 (48, 49). Likewise, AMPA receptor (AMPAR) inhibition with cyanquixaline injection in M1 cortex reduced motor skill retention (32). Consistent with the effect of GR-PO_4 deletion, a stable deficit of motor skill retention was also found after ablation of Drd1 neurons in dorsolateral striatum during consolidation (50). D1/D5 antagonist or dopamine depletion in motor cortex increased spine elimination and decreased spine survival in motor cortex, such as in the KI mice (51). In fact, D5 controls AMPA currents in motor cortex by promoting GluA1 PO_4, such as GR-PO_4 (52, 53). The similarities with the effect of GR-PO_4 deletion suggest that maintenance of the synaptic memory engram depends on GR-PO_4 and dopamine signaling to AMPAR, which will need further studies.

Physiological consequences of the BDNF-Val66Met allele, like those of GR-PO_4 deletion, are revealed not in the basal state but in response to experience-driven increase of neural activity

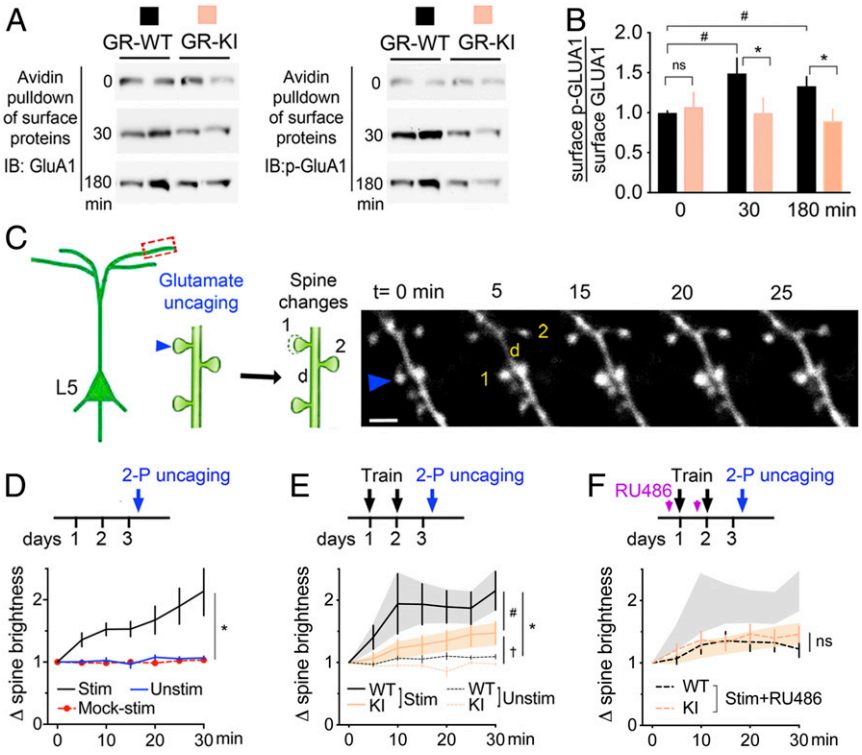

Fig. 5. GR-PO_4 is required for training-evoked spine maturation. (*A*) Avidin pulldown of biotinylated proteins from primary neurons at day in vitro 14 electroporated with GR-WT or GR-KI at day in vitro 0, and stimulated with 25 ng/mL BDNF and 1 μM dexamethasone for the indicated time. Each column of the immunoblot (IB) for for GluA1 and p-GluA1 represents an independent sample. (*B*) Surface GluA1-PO_4/GluA1 in cortical neurons expressing GR-WT or GR-KI. Mean ± SEM of $n = 11$ WT mice and $n = 8$ KI mice per group; two-way ANOVA: effect of mutant ($F_{1,53} = 6.61$, $P = 0.016$). Pairwise group comparison by unpaired *t* test (*$P < 0.05$, $^{\#}P < 0.001$). ns, not significant. (*C*) In vivo two-photon uncaging of 20 mM MNI-glutamate (90 iterations per laser at 720 nm, 0.7 mW, 0.1 Hz) in Hepes buffer in M1. The arrow indicates photostimulated spine (1) compared with the underlying dendritic shaft (d) and neighboring unstimulated spine (2). (Scale bar, 3 μm). (*D*) Specificity of glutamate-evoked spine enlargement normalized to baseline spine size in WT mice. Mean ± SEM of $n = 10$ stimulated (Stim) spines, $n = 9$ mock-stimulated spines (Mock-stim), and $n = 20$ neighbor spines (Unstim) in three mice; two-way ANOVA: effect of stimulation ($F_{2,237} = 83.9$, $P < 0.0001$) and time ($F_{6,237} = 6.78$, $P < 0.0001$), post hoc Tukey test (*$P < 0.0001$). (*E*) Effect of genotype on glutamate-evoked spine enlargement after 2 d of rotarod training. Mean ± SEM of $n = 23$ stimulated spines WT, $n = 40$ stimulated spines KI, $n = 18$ neighbor spines WT, and $n = 20$ neighbor spines KI in four mice per group; two-way ANOVA: effect of stimulation ($F_{3,631} = 21.93$, $P < 0.0001$) and time ($F_{6,631} = 2.43$, $P = 0.024$), post hoc Tukey test ($^{\#}P < 0.0001$, *$P < 0.0001$, $^{\dagger}P = 0.009$). (*F*) Effect of RU486 (20 mg/kg i.p. 20 min before each training session) on glutamate-evoked spine enlargement. Mean ± SEM of $n = 17$ stim+RU486 WT spines, $n = 13$ stim+RU486 KI spines in three mice; two-way ANOVA: effect of stimulation ($F_{3,605} = 10.13$, $P < 0.0001$) and time ($F_{6,605} = 3.96$, $P = 0.0007$). 2-P, two-photon.

(28, 54). This indicates that GR senses and responds to BDNF by selective GR-PO_4 that alters its activity and promotes learning and memory. Whether this reflects changes in GR genomic and/or nongenomic activity remains to be determined. Evidence obtained from RU486 injections indicates that GR-PO_4 signaling is required hours rather than minutes before dendritic spine maturation via a glutamate-dependent mechanism. Therefore, these effects depend on a slow process, likely genomic, to consolidate new spines. This could have implications for the encoding and persistence of new structural engrams required for adaptive plasticity that either translate to a new behavior or adapt to a changing environment (i.e., stress, learning, enrichment).

Our findings also have translational implications. Imbalances in the integration of BDNF-GR signaling axes would be predicted to trigger maladaptive processes that contribute to the pathophysiology observed in many neurological and other diseases (18, 24, 43, 55). For example, GR insufficiency is associated with a state of low BDNF levels in diseases presenting an activated inflammatory system that is relevant for patients with major depression, schizophrenia, glucocorticoid resistance syndrome, and Alzheimer's disease (56–59). Antidepressant therapies that successfully increase BDNF levels also correct GR-PO_4 and GR sensitivity (23, 60). GR-PO_4 has been suggested to be a mechanism contributing to glucocorticoid resistance in multiple disease models (61). Although many GR-PO_4 sites are glucocorticoid-dependent (18), our data indicate that GR-PO_4 can also be glucocorticoid-independent. This implies that GR activity is influenced by contextual signals in addition to glucocorticoids (22, 26, 62). This applies, for example, to the maintenance of sensory motor engrams as long as activity-dependent BDNF secretion and glucocorticoid oscillatory pulses are synchronized and stimulate the GR-PO_4 pathway. For that reason, aligning glucocorticoid treatment to neurotrophin release should be considered to promote neuroplasticity for sensory motor rehabilitation.

Methods

All experiments were carried out in accordance with the Directive by the Council of the European Communities (86/609/EEC). All protocols complied with the French Ministry of Research institutional guidelines (approved protocol 00651.01) and ethics committee at the University of Montpellier for the care and use of laboratory animals. All tools are listed in *SI Appendix*, Table S1.

Animals. The PO_4-deficient GR mouse (Flex GR-A152/A284 KI; Ozgene, Pty. Ltd.) was generated in a C57Bl6 background and crossed with the constitutive ROSA26-FLP line [*Gt(ROSA)26Sor*$^{tm2(FLP)Sor}$] to remove the neomycin cassette and the constitutive ROSA26-CRE line [*Gt(ROSA)26Sor*^{tm1Sor}] to produce a general deletion of GR-PO_4 sites (details are provided in *SI Appendix*, Fig. S1). Thy1-YFP transgenic mice [*B6.Cg-Tg(Thy1-YFP)HJrs/J*], BDNF-Val66Met

mice [*Bdnf*^{tm1Flee}, MGI:3664862], and WT mice in C57BL6 background (The Jackson Laboratory) were housed under a 12-h light/dark cycle (on 6:00 AM, off 6:00 PM) with unrestricted access to food and water. Chronic unpredictable mild stress includes one of the following daily random stressors (wet bedding, no bedding, food deprivation, crowded cage, 2-h or 6-h restraint, tilted cage, shaking, 24-h light cycle, forced swim, or tail suspension) for 10 consecutive days. Enrichment consisted of larger cages with toys of various colors and textures (tubes, tunnels, ladders, Lego pieces, beads, or nest) for 10 consecutive days. Homozygous males produced by heterozygous breeding schemes were used in all protocols. All efforts were made to minimize animal suffering and to reduce the number of mice utilized in each experiment.

Open Field. One-month-old mice freely explored an arena (50 cm × 50 cm) for 10-min video-recorded sessions, and total distance traveled was determined with Ethovison XT software (Noldus). Thigmotaxis represents the time spent in the center of the arena (29 cm × 29 cm).

Elevated Plus Maze. Mice at 3 mo of age freely explored the arms (elevation of 50 cm × 50 cm × 20 cm) for 10-min video-recorded sessions to score the number of entries and time spent in each arm.

Forced Swim. Mice at 3 mo of age were subjected to a forced swim test for 9 min in a beaker (15 cm × 25 cm) filled with tap water at room temperature during the stress protocol [once a week between postnatal day (PNDs) 23 and 36], and the trial was video-recorded. Trial data represent an acquired behavioral response in the stress groups but a novel response in the control groups reared in standard conditions.

Tail Suspension. Mice at 3 mo of age were subjected to a video-recorded tail suspension test for 6 min during the stress protocol (once a week between PNDs 23 and 36). Trial data represent an acquired behavioral response in the stress groups but a novel response in the control groups reared in standard conditions (63).

Motor Learning. Mice were habituated for 30 min (15 trials) on the nonaccelerating rotarod (2 rpm for 1 min, followed by 30-s rest intertrials) for two consecutive days at glucocorticoid circadian oscillation peak (7:00 PM in darkness) before two training sessions of 1 h also at 7:00 PM in darkness. Training consisted in 15 trial sessions on the accelerated rod (from 2 to 80 rpm reached in 2 min with 1-min rest intertrials) for two consecutive days. Control mice are habituated and trained on a slow accelerating rod (2 rpm) that did induce spine patterning in the motor cortex. To characterize training-induced c-Fos expression, mice were euthanized 45 min after training at 80 rpm (trained group) or 2 rpm (untrained group). Motor performance is indexed as latency to fall. Acquisition is calculated as performance improvement index = mean $d_2(t_{14} + t_{15})$ − mean $d_1(t_1 + t_2)$. Retention on recall (7:00 PM) is calculated as motor skill retention index = improvement index − [mean $d_{14}(t_1 + t_2)$ − mean $d_1(t_1 + t_2)$], where d is the day at testing and t is the trial number.

Transcranial Two-Photon Microscopy. Mice were anesthetized with a mix of ketamine/xylazine (0.075 mg/g and 0.01 mg/g, respectively) before surgery. Thin-skull preparation for transcranial in vivo imaging in motor cortex (coordinates from bregma −1.3 mm, +1.2 mm lateral) was preferred to open-skull preparation because it prevents artifacts due to surgically induced chronic inflammation (64). All images were acquired with a Zeiss LSM710 two-photon microscope coupled to a Ti:sapphire laser tuned to 920 nm (Spectra Physics) and a water immersion 20× objective (1.0 numerical aperture, Apocromat; Carl Zeiss). Laser power was kept below 5 mW to avoid photodamage. Images were taken at each image session for each mouse using 70 μm × 70 μm (512 × 512 pixels) at a 0.75-μm step with a scanning dwell time of 2.55 μs per pixel.

Reimaging of the Same Field of View. Repeat imaging of the same dendritic field before (image 1 at PND23) and after (image 2 at PND26) training, as well as at recall (image 3 at PND36), offers an opportunity to identify a synaptic engram of motor skill training that correlates with motor performance (25). Comparison of pairs of images identified stable spines (present in images 1, 2, and 3), eliminated spines (present in image 1 but not in image 2 and/or 3), formed spines (present in image 2 but not in image 1), and survival of new spines (present in images 2 and 3 but not in image 1), as well as preexisting old spines (present in image 1 but not in image 2 or 3). To this end, a detailed map of the pial vasculature was taken for subsequent relocation. Bone regrowth between imaging sessions is thinned using disposable ophthalmic surgical blades (Surgistar). The skull is further thinned between imaging sessions down to 18–20 μm, allowing no more than four consecutive sessions to avoid cracking the skull (65). The scalp is sutured and topped with topical antibiotic cream.

Time-Lapse Imaging Through a Cranial Window. Two-photon microscopy was performed in open-skull preparations to facilitate access of drugs to the pial surface of cortex after surgical removal of meninges covered by a thin layer of low-melting-point agarose [1.5% in Hepes-buffered artificial cerebrospinal fluid (ACSF)] to avoid heartbeat motion artifacts. Baseline spine dynamics were captured in Hepes-buffered ACSF [120 mM NaCl, 3.5 mM KCl, 0.4 mM KH_2PO_4, 15 mM glucose, 1.2 mM $CaCl_2$, 5 mM $NaHCO_3$, 1.2 mM Na_2SO_4, Hepes (pH 7.4)] for 5 min. Prior glutamate uncaging was performed in Hepes-buffered ACSF with 20 mM MNI-glutamate (Sigma) photostimulated with 90 iterations at 0.1 Hz of 5% laser power tuned to 720 nm (0.7 mW) as described (66). The success rate of spine enlargement was calculated as the number of trials in which spine brightness exceeded 10% of the initial value divided by the total number of trials.

Image Analysis. All images obtained from time-lapse imaging sessions were realigned with the ImageJ plug-in RegStack to minimize artifacts of heartbeat pulsations. Images were stitched together using ImageJ. Image stacks between sessions were compared using ImageJ. Dendritic segments included in the analyses met the following criteria: (*i*) Segments were parallel or at acute angles relative to the coronal surface of sections to allow unambiguous identification of spines, (*ii*) segments had no overlap with other branches, and (*iii*) segments from the apical tree were imaged within the first 100 μm from the pial surface. About 200 dendritic spines from at least 20–30 dendritic segments were counted per condition throughout the imaging sessions and averaged per animal. For this study, more than 23,000 spines were tracked in time-lapse images (three to five time points). The resolution of our three-dimensional images is insufficient to resolve spines reliably in the *z* axis. So, spines below or above dendrites were not analyzed. All clear protrusions emanating laterally from the dendritic shaft, irrespective of apparent shape, were counted. Spines were considered deleted if they disappeared into the haze of the dendrites (less than five pixels in length); spines were considered formed if they clearly protruded from the dendrites (five or more pixels in length). To calculate spine brightness, the pixel values containing the spine head were summed. Background fluorescence, calculated over the same-sized box adjacent to the spine, was subtracted. Since dendritic shaft diameters were constant and relatively uniform, we used them to correct fluorescence levels. Average shaft pixel intensity was calculated over the same-sized box adjacent to the spine. The background-subtracted pixel value for each spine was divided by the average shaft pixel value as previously described (67). The resulting relative brightness is expected to be proportional to the spine volume. The fraction of spines gained subtracted of the spines lost between imaging sessions, was calculated as the net ratio = $(N_{formed} - N_{deleted})/(2 \times N_{total})$, where *N* is the population size of spines.

Live Slice Preparation. Mice were decapitated at PDN26, 12–15 h after the last training session as described (39), and brains were immersed in ice-cold oxygenated (95% O_2, 5% CO_2) ACSF containing 127.25 mM NaCl, 1.75 mM KCl, 1.25 mM KH_2PO_4, 1 mM $MgCl_2$, 2 mM $CaCl_2$, 26 mM $NaHCO_3$, and 10 mM glucose. Coronal slices (400 μm), including the M1 area (1.5–3.5 mm anterior to bregma, 2–4 mm lateral), were transferred to a temperature-controlled (34 ± 1 °C) interface chamber and perfused with oxygenated ACSF at a rate of 1 mL·min^{-1}. Slices were allowed to recover for at least 1 h before recordings.

Electrophysiological Recordings. Stimulation electrodes were positioned in L2/3, 1.5–1.8 mm lateral to the midline, and recording electrodes were placed 500 μm laterally. Field potentials were evoked by stimulation of 0.2 ms at 0.03 Hz. For induction of LTP, stimulus intensity eliciting 50% of the maximum amplitude was used for all measurements before and after LTP induction paired with a touch application of bicuculline methiodide (3.5 mM, gamma-aminobutyric acid type A antagonist) as described (33). Baseline amplitudes were recorded using single stimuli applied every 30 s. Following a 30-min stable baseline period, LTP was induced by theta burst stimulation, consisting of 10 trains of 5-Hz stimuli, each composed of four (200-ms) pulses at 100 Hz, repeated five times every 10 s. Maximum LTP values are expressed as a percentage of baseline. Neural pathways were considered saturated if the difference between two states of LTP inductions in the habituated and trained mice was not significantly different ($P > 0.5$). The magnitude of occlusion of LTP-like plasticity was calculated as occlusion index = [d_2(LTP$_1$-baseline) − mean d_0(LTP$_1$-baseline)] + [d_2(LTP$_2$-LTP$_1$) − mean d_0(LTP$_2$-LTP$_1$)] + [d_2(LTP$_3$-LTP$_2$) − mean d_0(LTP$_3$-LTP$_2$)], where d_0 is after 2 d of habituation (2 rpm) and d_2 is after 2 d of training (80 rpm).

Immunohistochemistry. Mice were anesthetized at PDN26 or PDN36 with pentobarbital [50 mg/kg intraperitoneal (i.p.); Ceva santé Animale] and perfused at a rate of 3 mL·min^{-1} through the ascending aorta with 30 mL of ice-cold 0.9% NaCl before decapitation. Brain hemisections were fixed with 4% ice-cold paraformaldehyde for 2 h and sectioned with a vibratome. Free-floating coronal sections rinsed in phosphate-buffered saline (PBS) were blocked in 3% normal donkey serum, PBS, and 0.1% Triton X-100 for 2 h at 25 °C. Antibodies are listed in *SI Appendix*, Table S1. Images were acquired with a confocal microscope (LSM780; Carl Zeiss) and 10× and 20× dry objectives and a 40× oil-immersion objective to capture dendrites spine for counting densities. Excitation and acquisition parameters were unchanged during the acquisition of all images. More than 26,000 NG neurons, 7,000 PV neurons, 24,000 GR cells, and 2,200 Thy1-YFP neurons were counted in all groups to determine the proportions of cells colabeled with c-Fos and GR-PO_4.

Synaptosome Preparation. Mice were anesthetized at PDN26 with pentobarbital (50 mg/kg i.p.; Ceva santé Animale) and perfused at a rate of 3 mL·min^{-1} through the ascending aorta with 30 mL of 0.9% NaCl before decapitation. Motor cortex from brain hemisections was harvested from 200-μm-thick sections dissected with a tissue punch (Stoelting Co.). Potter was used to make homogenates in ice-cold 0.32 M sucrose, 1 mM ethylenediaminetetraacetic acid (EDTA), 10 mM Hepes (pH 8), and 1 mg/mL bovine serum albumin (BSA) complemented with protease and phosphatase inhibitors, and centrifuged twice (1,000 × *g* for 1 min) to clear debris. Particles were centrifuged (14,000 × *g* for 12 min), and pellets were suspended in ice-cold 45% Percoll diluted in 140 mM NaCl, 5 mM KCl, 25 mM Hepes (pH 8.0), 1 mM EDTA, and 10 mM glucose plus inhibitors. Synaptosome fractions were collected at the surface after centrifugation (14,000 × *g* for 2 min) and rinsed in ice-cold 0.32 M sucrose, 1 mM EDTA, and 10 mM Hepes (pH 8). After centrifugation (14,000 × *g* for 12 min), synaptosomes were lysed in 2% sodium dodecyl sulfate (SDS).

DNA Transfection. In utero electroporations [30 V; pON, 50 ms; pOFF, 950 ms; five pulses with NEPA21 (Nepagene); 1 μg of DNA] were performed at embryonic day 15 on mouse embryos and newborns developed for 1 mo of age (23). Mice were anesthetized with 4% isoflurane/oxygen and maintained at 1.5–2% isoflurane (Abbott Laboratories) throughout surgery using TEC3N (Anesteo). Mice received preemptive analgesia with lidocaine (Xylovet, 3.5 mg/kg at incision site). A subcutaneous injection of the analgesic buprenorphine (Buprecare, 0.05 mg/kg) was administered postsurgery and the next day. In vitro electroporations were performed with the AMAXA system. Plasmids electroporated consist of DNA vectors for molecular replacement of endogenous GR by the short hairpin RNA-resistant PO_4-deficient GR (GR-2A: S152A/S284A) or GR-WT as previously described (30).

Cell Culture and Biotinylation Assay. Primary embryonic day 18 cortical neurons prepared from time-pregnant C57BL6 mice were cultured on poly-D-lysine and maintained for 2 wk in vitro in neurobasal medium containing B27 supplement, 0.5 mM L-glutamine, 10 μM 5-fluorouridine, and 10 μM uridine. Cells were rinsed three times with PBS containing 1 mM $CaCl_2$ and 0.5 mM $MgCl_2$, and were incubated successively at 4 °C with sulfo-NHS-acetate (Pierce) to block surface proteins; with 100 mM glycine to quench reaction; at 37 °C for the indicated time in the presence of 25 ng/mL BDNF and 1 μM dexamethasone; and, finally, at 4 °C with sulfo-NHS-LC-biotin (Pierce) to label newly inserted surface proteins. Cells were lysed in 10 mM Tris·HCl (pH 8), 150 mM NaCl, 1 mM EDTA, 10% glycerol, 1% Nonidet P-40, and 0.1% SDS plus protease inhibitors, and were cleared by centrifugation (12,000 × *g* for 10 min). Streptavidin-agarose pulldown (Pierce) permitted purification of biotinylated surface proteins further rinsed five times with radioimmunoprecipitation assay buffer and resolved in 10% SDS/polyacrylamide gel electrophoresis.

Western Blot. Protein concentrations were measured with a bicinchoninic acid assay against BSA standards (Thermo Fisher Scientific) using a plate reader for measuring absorbance (Tecan). Immunoreactivities (antibodies are listed in *SI Appendix*, Table S1) were revealed by chemiluminescence (GE Healthcare) and densitometric analysis of grayscale digital images using Chemidoc Touch (Bio-Rad Laboratories).

Statistics. Parameters used to quantify imaging data include the following: (*i*) formation/deletion/survival of dendritic spines, (*ii*) density of dendritic spines, (*iii*) spine head diameter, (*iv*) double-labeled cells, (*v*) and cortical layers visualized with 4′,6-diamidino-2-phenylindole stain and Thy1-YFP in L5. Parameters used to quantify motor performance data include the following: (*i*) latency to fall from the rotarod within-trials improvement as an index of learning and (*ii*) intertrial improvement as an index of retention. Representation of *N* for each dataset is indicated in the figure legends. All data collected in animals were from littermate controls and were averaged per experimental group. We used the Student's *t* test to compare two groups or time points and Pearson correlation for linear associations between datasets with Prism 8.0 software (GraphPad). We used factorial ANOVA to compare multiple groups (training, genotype, stress, and enrichment), followed by post hoc pairwise comparison with the Tukey test for corrections. All data are shown as mean ± SEM. Significance level is set at $\alpha \leq 0.05$. No data were removed from analyses, including statistical outliers. Estimates of sample size were calculated by power analysis based on preliminary data. Sample size was chosen to ensure 80% power to detect the prespecified effect size. Preestablished criteria for stopping data collection included the following: (*i*) mice reaching ethical endpoint limits, (*ii*) unexpected mortality (e.g., anesthesia), (*iii*) crack of the thin skull preparation that would cause unwanted inflammation, and (*iv*) brains badly perfused and unusable for histology.

ACKNOWLEDGMENTS. We thank F. S. Lee (Weill Cornell Medical School) for providing the Val66Met mice and W. B. Gan (New York University School of Medicine), C. Liston (Weill Cornell Medical School), and C. Lafont (Imagerie du Petit Animal de Montpellier) for their advice on two-photon microscopy. This work is supported by INSERM/AVENIR (F.J.), FP7 Marie Curie (F.J.), Montpellier University (F.J.), the Fondation pour la recherche médicale (F.J.), and NIH Grant R56MH115281 (to M.J.G. and F.J.).

1. S. J. Lupien, B. S. McEwen, M. R. Gunnar, C. Heim, Effects of stress throughout the lifespan on the brain, behaviour and cognition. *Nat. Rev. Neurosci.* **10**, 434–445 (2009).
2. C. Finsterwald, C. M. Alberini, Stress and glucocorticoid receptor-dependent mechanisms in long-term memory: From adaptive responses to psychopathologies. *Neurobiol. Learn. Mem.* **112**, 17–29 (2014).
3. L. Schwabe, M. Joëls, B. Roozendaal, O. T. Wolf, M. S. Oitzl, Stress effects on memory: An update and integration. *Neurosci. Biobehav. Rev.* **36**, 1740–1749 (2012).
4. M. Fu, Y. Zuo, Experience-dependent structural plasticity in the cortex. *Trends Neurosci.* **34**, 177–187 (2011).
5. C. R. Bramham, Local protein synthesis, actin dynamics, and LTP consolidation. *Curr. Opin. Neurobiol.* **18**, 524–531 (2008).
6. J. Tanaka *et al.*, Protein synthesis and neurotrophin-dependent structural plasticity of single dendritic spines. *Science* **319**, 1683–1687 (2008).
7. T. Xu *et al.*, Rapid formation and selective stabilization of synapses for enduring motor memories. *Nature* **462**, 915–919 (2009).
8. G. Yang, F. Pan, W. B. Gan, Stably maintained dendritic spines are associated with lifelong memories. *Nature* **462**, 920–924 (2009).
9. L. Ma *et al.*, Experience-dependent plasticity of dendritic spines of layer 2/3 pyramidal neurons in the mouse cortex. *Dev. Neurobiol.* **76**, 277–286 (2016).
10. C. C. Chen, J. Lu, Y. Zuo, Spatiotemporal dynamics of dendritic spines in the living brain. *Front. Neuroanat.* **8**, 28 (2014).
11. K. P. Berry, E. Nedivi, Spine dynamics: Are they all the same? *Neuron* **96**, 43–55 (2017).
12. A. E. Autry, L. M. Monteggia, Brain-derived neurotrophic factor and neuropsychiatric disorders. *Pharmacol. Rev.* **64**, 238–258 (2012).
13. S. C. Harward *et al.*, Autocrine BDNF-TrkB signalling within a single dendritic spine. *Nature* **538**, 99–103 (2016).
14. F. Jeanneteau, M. V. Chao, "Neurotrophins and synaptogenesis" in *Cellular Migration and Formation of Neuronal Connections: Comprehensive Developmental Neuroscience*, J. Rubenstein, P. Rakic, Eds. (Elsevier, ed. 2, 2013), pp. 639–659.
15. J. Wook Koo *et al.*, Essential role of mesolimbic brain-derived neurotrophic factor in chronic social stress-induced depressive behaviors. *Biol. Psychiatry* **80**, 469–478 (2016).
16. E. G. Pitts, D. C. Li, S. L. Gourley, Bidirectional coordination of actions and habits by TrkB in mice. *Sci. Rep.* **8**, 4495 (2018).
17. E. T. Barfield, S. L. Gourley, Prefrontal cortical trkB, glucocorticoids, and their interactions in stress and developmental contexts. *Neurosci. Biobehav. Rev.* **95**, 535–558 (2018).
18. F. Jeanneteau, A. Borie, M. Chao, M. Garabedian, Bridging the gap between brain-derived neurotrophic factor and glucocorticoid effects on brain networks. *Neuroendocrinology* 10.1159/000496392 (2018).
19. M. F. Egan *et al.*, The BDNF val66met polymorphism affects activity-dependent secretion of BDNF and human memory and hippocampal function. *Cell* **112**, 257–269 (2003).
20. H. Yu *et al.*, Variant brain-derived neurotrophic factor Val66Met polymorphism alters vulnerability to stress and response to antidepressants. *J. Neurosci.* **32**, 4092–4101 (2012).
21. I. Shalev *et al.*, BDNF Val66Met polymorphism is associated with HPA axis reactivity to psychological stress characterized by genotype and gender interactions. *Psychoneuroendocrinology* **34**, 382–388 (2009).
22. W. M. Lambert *et al.*, Brain-derived neurotrophic factor signaling rewrites the glucocorticoid transcriptome via glucocorticoid receptor phosphorylation. *Mol. Cell. Biol.* **33**, 3700–3714 (2013).

23. M. Arango-Lievano *et al*., Neurotrophic-priming of glucocorticoid receptor signaling is essential for neuronal plasticity to stress and antidepressant treatment. *Proc. Natl. Acad. Sci. U.S.A.* **112**, 15737–15742 (2015).
24. B. S. McEwen, Preserving neuroplasticity: Role of glucocorticoids and neurotrophins via phosphorylation. *Proc. Natl. Acad. Sci. U.S.A.* **112**, 15544–15545 (2015).
25. C. Liston *et al*., Circadian glucocorticoid oscillations promote learning-dependent synapse formation and maintenance. *Nat. Neurosci.* **16**, 698–705 (2013).
26. M. Arango-Lievano, F. Jeanneteau, Timing and crosstalk of glucocorticoid signaling with cytokines, neurotransmitters and growth factors. *Pharmacol. Res.* **113**, 1–17 (2016).
27. R. M. Zanca *et al*., Environmental enrichment increases glucocorticoid receptors and decreases GluA2 and protein kinase M zeta (PKMζ) trafficking during chronic stress: A protective mechanism? *Front. Behav. Neurosci.* **9**, 303 (2015).
28. B. Fritsch *et al*., Direct current stimulation promotes BDNF-dependent synaptic plasticity: Potential implications for motor learning. *Neuron* **66**, 198–204 (2010).
29. A. Hayashi-Takagi *et al*., Labelling and optical erasure of synaptic memory traces in the motor cortex. *Nature* **525**, 333–338 (2015).
30. M. Arango-Lievano *et al*., Deletion of neurotrophin signaling through the glucocorticoid receptor pathway causes tau neuropathology. *Sci. Rep.* **6**, 37231 (2016).
31. S. A. McHughen *et al*., BDNF val66met polymorphism influences motor system function in the human brain. *Cereb. Cortex* **20**, 1254–1262 (2010).
32. H. Kida *et al*., Motor training promotes both synaptic and intrinsic plasticity of layer II/III pyramidal neurons in the primary motor cortex. *Cereb. Cortex* **26**, 3494–3507 (2016).
33. M. S. Rioult-Pedotti, D. Friedman, J. P. Donoghue, Learning-induced LTP in neocortex. *Science* **290**, 533–536 (2000).
34. G. Cantarero, A. Lloyd, P. Celnik, Reversal of long-term potentiation-like plasticity processes after motor learning disrupts skill retention. *J. Neurosci.* **33**, 12862–12869 (2013).
35. S. J. Martin, R. G. Morris, Cortical plasticity: It's all the range! *Curr. Biol.* **11**, R57–R59 (2001).
36. R. Malinow, R. C. Malenka, AMPA receptor trafficking and synaptic plasticity. *Annu. Rev. Neurosci.* **25**, 103–126 (2002).
37. H. K. Lee, M. Barbarosie, K. Kameyama, M. F. Bear, R. L. Huganir, Regulation of distinct AMPA receptor phosphorylation sites during bidirectional synaptic plasticity. *Nature* **405**, 955–959 (2000).
38. A. S. Kristensen *et al*., Mechanism of Ca2+/calmodulin-dependent kinase II regulation of AMPA receptor gating. *Nat. Neurosci.* **14**, 727–735 (2011).
39. R. Padmashri, B. C. Reiner, A. Suresh, E. Spartz, A. Dunaevsky, Altered structural and functional synaptic plasticity with motor skill learning in a mouse model of fragile X syndrome. *J. Neurosci.* **33**, 19715–19723 (2013).
40. F. Jeanneteau *et al*., A functional variant of the dopamine D3 receptor is associated with risk and age-at-onset of essential tremor. *Proc. Natl. Acad. Sci. U.S.A.* **103**, 10753–10758 (2006).
41. K. J. Harms, M. S. Rioult-Pedotti, D. R. Carter, A. Dunaevsky, Transient spine expansion and learning-induced plasticity in layer 1 primary motor cortex. *J. Neurosci.* **28**, 5686–5690 (2008).
42. M. Zhao *et al*., BDNF Val66Met polymorphism, life stress and depression: A meta-analysis of gene-environment interaction. *J. Affect. Disord.* **227**, 226–235 (2018).
43. F. Jeanneteau, M. V. Chao, Are BDNF and glucocorticoid activities calibrated? *Neuroscience* **239**, 173–195 (2013).
44. L. H. L. Ng *et al*., Ketamine and selective activation of parvalbumin interneurons inhibit stress-induced dendritic spine elimination. *Transl. Psychiatry* **8**, 272 (2018).
45. C. C. Chen, J. Lu, R. Yang, J. B. Ding, Y. Zuo, Selective activation of parvalbumin interneurons prevents stress-induced synapse loss and perceptual defects. *Mol. Psychiatry* **23**, 1614–1625 (2018).
46. K. Chen *et al*., Treadmill exercise suppressed stress-induced dendritic spine elimination in mouse barrel cortex and improved working memory via BDNF/TrkB pathway. *Transl. Psychiatry* **7**, e1069 (2017).
47. T. C. Hill, K. Zito, LTP-induced long-term stabilization of individual nascent dendritic spines. *J. Neurosci.* **33**, 678–686 (2013).
48. H. Makino, R. Malinow, AMPA receptor incorporation into synapses during LTP: The role of lateral movement and exocytosis. *Neuron* **64**, 381–390 (2009).
49. E. Y. Yuen *et al*., Repeated stress causes cognitive impairment by suppressing glutamate receptor expression and function in prefrontal cortex. *Neuron* **73**, 962–977 (2012).
50. P. F. Durieux, S. N. Schiffmann, A. de Kerchove d'Exaerde, Differential regulation of motor control and response to dopaminergic drugs by D1R and D2R neurons in distinct dorsal striatum subregions. *EMBO J.* **31**, 640–653 (2012).
51. L. Guo *et al*., Dynamic rewiring of neural circuits in the motor cortex in mouse models of Parkinson's disease. *Nat. Neurosci.* **18**, 1299–1309 (2015).
52. L. Froux *et al*., D5 dopamine receptors control glutamatergic AMPA transmission between the motor cortex and subthalamic nucleus. *Sci. Rep.* **8**, 8858 (2018).
53. X. Sun, Y. Zhao, M. E. Wolf, Dopamine receptor stimulation modulates AMPA receptor synaptic insertion in prefrontal cortex neurons. *J. Neurosci.* **25**, 7342–7351 (2005).
54. J. A. Kleim *et al*., BDNF val66met polymorphism is associated with modified experience-dependent plasticity in human motor cortex. *Nat. Neurosci.* **9**, 735–737 (2006).
55. N. P. Daskalakis, E. R. De Kloet, R. Yehuda, D. Malaspina, T. M. Kranz, Early life stress effects on glucocorticoid-BDNF interplay in the hippocampus. *Front. Mol. Neurosci.* **8**, 68 (2015).
56. D. W. Cain, J. A. Cidlowski, Specificity and sensitivity of glucocorticoid signaling in health and disease. *Best Pract. Res. Clin. Endocrinol. Metab.* **29**, 545–556 (2015).
57. R. A. Quax *et al*., Glucocorticoid sensitivity in health and disease. *Nat. Rev. Endocrinol.* **9**, 670–686 (2013).
58. C. M. Pariante, Why are depressed patients inflamed? A reflection on 20 years of research on depression, glucocorticoid resistance and inflammation. *Eur. Neuropsychopharmacol.* **27**, 554–559 (2017).
59. M. J. Garabedian, C. A. Harris, F. Jeanneteau, Glucocorticoid receptor action in metabolic and neuronal function. *F1000 Res.* **6**, 1208 (2017).
60. M. S. Lee *et al*., Temporal variability of glucocorticoid receptor activity is functionally important for the therapeutic action of fluoxetine in the hippocampus. *Mol. Psychiatry* **21**, 252–260 (2016).
61. A. J. Galliher-Beckley, J. A. Cidlowski, Emerging roles of glucocorticoid receptor phosphorylation in modulating glucocorticoid hormone action in health and disease. *IUBMB Life* **61**, 979–986 (2009).
62. A. J. Galliher-Beckley, J. G. Williams, J. A. Cidlowski, Ligand-independent phosphorylation of the glucocorticoid receptor integrates cellular stress pathways with nuclear receptor signaling. *Mol. Cell. Biol.* **31**, 4663–4675 (2011).
63. F. Jeanneteau *et al*., The stress-induced transcription factor NR4A1 adjusts mitochondrial function and synapse number in prefrontal cortex. *J. Neurosci.* **38**, 1335–1350 (2018).
64. M. Arango-Lievano *et al*., Topographic reorganization of cerebrovascular mural cells under seizure conditions. *Cell Rep.* **23**, 1045–1059 (2018).
65. M. Arango-Lievano, P. Giannoni, S. Claeysen, N. Marchi, F. Jeanneteau, Longitudinal in vivo imaging of the cerebrovasculature: Relevance to CNS diseases. *J. Vis. Exp.*, 10.3791/54796 (2016).
66. J. Noguchi *et al*., In vivo two-photon uncaging of glutamate revealing the structure-function relationships of dendritic spines in the neocortex of adult mice. *J. Physiol.* **589**, 2447–2457 (2011).
67. A. J. Holtmaat *et al*., Transient and persistent dendritic spines in the neocortex in vivo. *Neuron* **45**, 279–291 (2005).

SUPPLEMENTAL INFORMATION

Arango-Lievano et al. "Persistence of learning-induced synapses depends on neurotrophic-priming of glucocorticoid receptors"

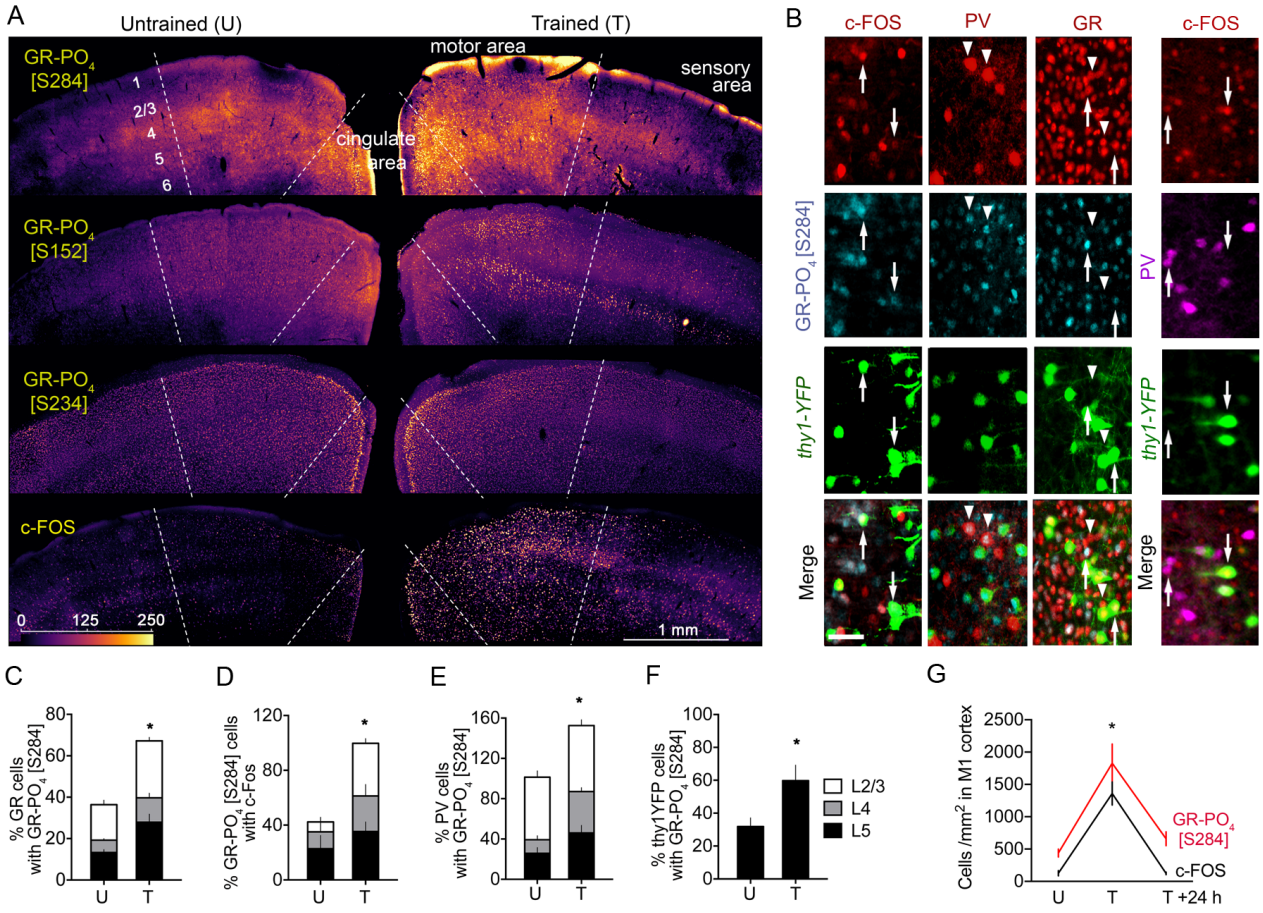

Figure S1. GR-PO$_4$ induction in neurons of motor cortex upon motor skills training on the rotarod.

(A) Expression heat map of GR-PO$_4$ isoforms (p-Ser284, p-Ser-152, p-Ser234) and c-FOS in motor areas of cortex 45 min after 2 days of training (T) or no training (U). Induction of GR-PO$_4$ (p-Ser284 and p-Ser-152) and c-FOS are most significant in the layers L2/3 and L5 of M1 cortex.

(B) Cell markers co-expressing GR-PO$_4$ and c-FOS in L5 of M1 cortex. Arrows indicate co-expression of markers. Motor training induced GR-PO$_4$ signaling in principal neurons as showed by triple labeling of thy1-YFP, GR-PO$_4$ and c-FOS in L5 M1 cortex. Motor training also induced GR-PO$_4$ and c-FOS in parvalbumin (PV) interneurons as showed by double labeling of PV, GR-PO$_4$ as well as PV and c-Fos in L5 M1 cortex. Scale=25 µm.

(C) Training induced GR-PO$_4$ in M1 cortex. Proportion of GR-PO$_4$ cells co-labeled with GR. Means ±SEM of n=7 mice/ group, 2-way ANOVA: Effect of training $F_{1,36}$=37.67, p<0.0001, post-hoc Sidak test *p<0.01.

(D) Training induced GR-PO$_4$ in cells that also express c-FOS in M1 cortex. Proportion of GR-PO$_4$ cells co-labeled with c-FOS. Means ±SEM of n=7 mice/ group, 2-way ANOVA: Effect of training $F_{1,36}$=12.34, p=0.0012, post-hoc Sidak test *p=0.0065.

(E) Proportion of PV neurons co-labeled with GR-PO_4. Means ±SEM of n=7 mice/ group, 2-way ANOVA: Effect of training $F_{1,36}$=13.7, p=0.0007, post-hoc Sidak test *p<0.05. Training induced GR-PO_4 in a substantial number of PV cells in M1 cortex.
(F) Proportion of thy1-YFP neurons co-labeled with GR-PO_4. Means ±SEM of n=7 mice/ group. Unpaired t-test: Effect of training $t_{(12)}$=2.59 *p=0.023. Training induced GR-PO_4 in a substantial number of principal thy1-YFP neurons in M1 cortex.
(G) Induction of GR-PO_4 and c-FOS 45 min after the last training on day 2 (T, n=5) and 24 hours post-training on day 3 (T+24h, n=4) compared to untrained mice sacrificed on day 2 (U, n=5). Means ±SD, 1-way ANOVA: Effect of training $F_{(5,22)}$=18.8, p<0.0001 post-hoc Sidak test *p<0.001.

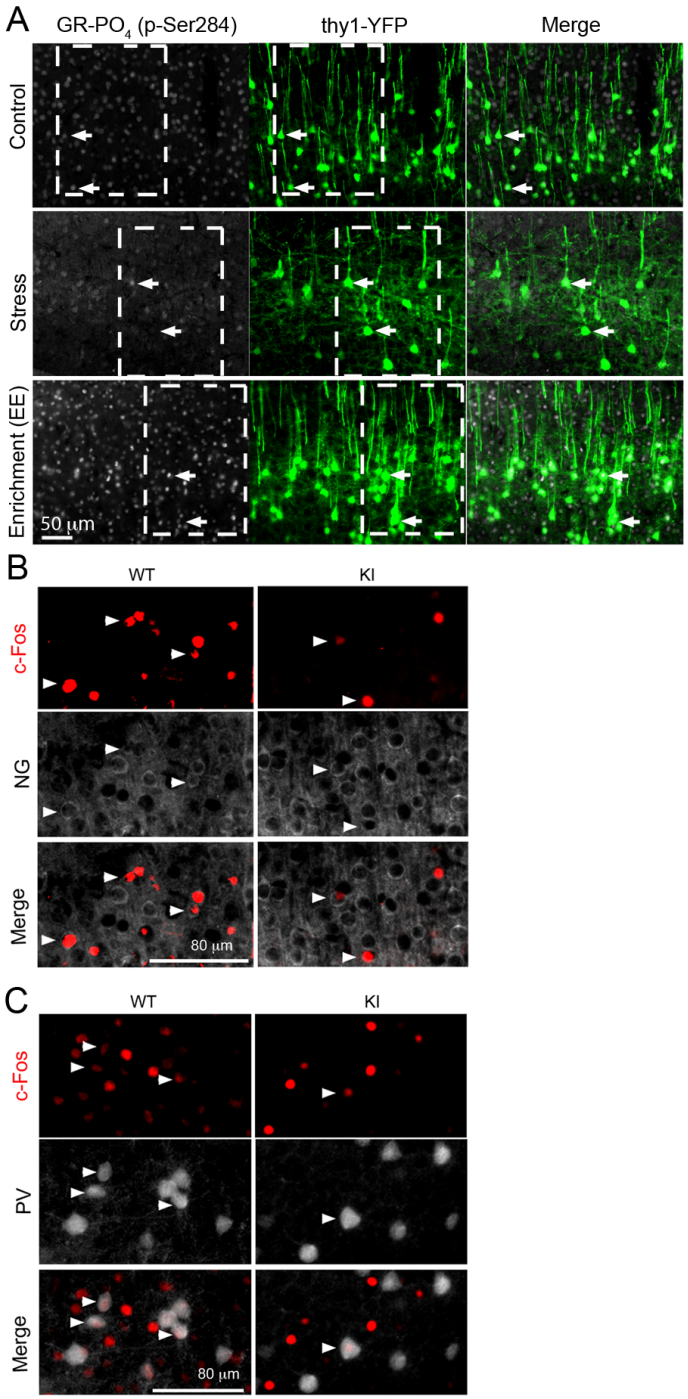

Figure S2. Induction of GR-PO_4 in motor cortex and effects of its deletion.
(A) Effect of stress and enrichment (EE) between postnatal day (PND)25 and PND36 immediately after the training on GR-PO_4 (p-Ser284) in the layer 5 in M1 cortex. Insets indicate the fields of view displayed in figure 1F.
(B) Induction of c-FOS in principal neurons marked with neurogranin (NG) in the layer 2/3 of the M1 cortex from WT and KI mice sacrificed 45 min after 2 days of training (15 trials each). This refers to Figure 1G.

(C) Induction of c-FOS in inhibitory neurons marked with parvalbumin (PV) in the layer 5 of the M1 cortex from WT and KI mice sacrificed 45 min after 2 days of training (15 trials each). This refers to Figure 1G.

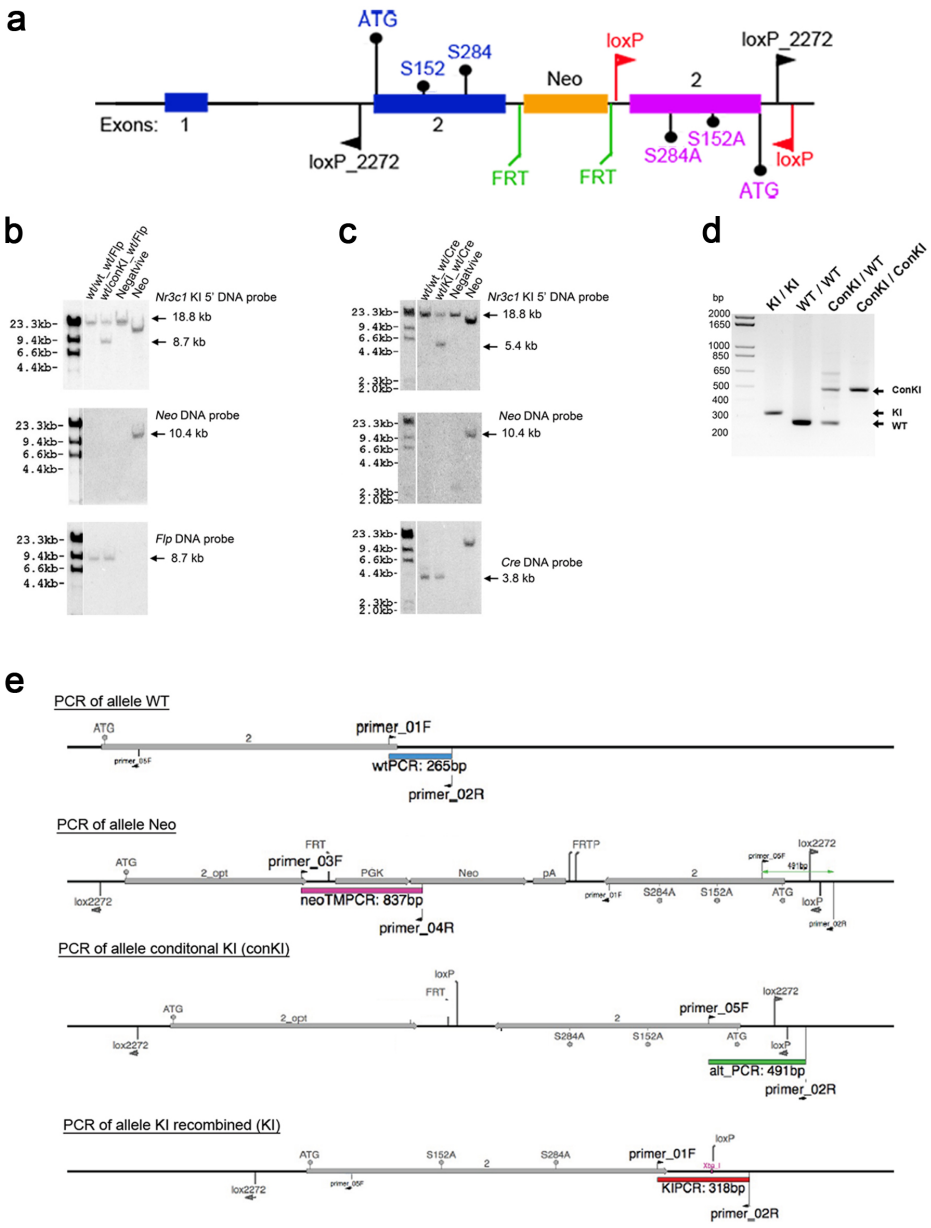

Figure S3. Knockin construct of PO_4-deficient GR mouse at sites responding to BDNF.
(a) N*r3c1* locus on chromosome 18 (chr18:39410545-39491301) (MGI:95824) presenting an exon 2 with S152 and S284 (WT) and another exon 2 with the mutations A152A and A284 (KI) in head-to-head orientation flanked by 2 pairs of loxP sites, both targets of the CRE recombinase. To avoid the formation of RNA duplex between both exon 2, the nucleic acid sequence of exon 2 WT has been engineered to deviate from the original (mus musculus C57Bl6) while maintaining the aminoacid sequence; the nucleic acid sequence of the exon 2 KI is the original with the exception of S152A and S284A mutations. The neomycin cassette served for the selection of ES clones (derived from C57Bl6 background) that integrated the construct. Selected clones were implanted in C57Bl6 recipient females. F1 were bred with C57Bl6 mice for transmission of the conditional allele (conKI) to the germline. Subsequent cross with constitutive FLP mouse line (ROSA26-FLP by Ozgene) permitted general deletion of the neo cassette. Subsequent cross with

constitutive CRE mouse line (ROSA26-CRE by Ozgene) permitted general replacement of WT exon by KI exon. Heterozygous F1 were bred with C57Bl6 mice for transmission of the recombined allele to the germline. Heterozygous F1 were bred with C57Bl6 mice to obtain mice harboring either a KI allele with normal nucleic acid sequence or an WT allele with normal nucleic acid sequence.
(b) Validation of recombination by Southern blot. Three DNA probes were used to ensure recombination of the allele in genomic DNA prior digested with BamHI. The *Nr3c1* 5' DNA probe detects the conKI allele, the *Neo* DNA probe detects the selection cassette and the *Flp* DNA probe detects the expression of the recombinase.
(c) Validation of recombination of the conKI allele by Southern blot. Three DNA probes were used to ensure recombination of the allele in genomic DNA prior digested with BamHI. The *Nr3c1* 5' DNA probe detects the conKI allele, the *Neo* DNA probe failed to detect the selection cassette removed in the previous generation, and the *CRE* DNA probe detects the expression of the recombinase.
(d) Typical result of genotyping by PCR of genomic DNA in 2% agarose gel electrophoresis. Specific bands are as follow: ConKI 491 bp, WT 265 bp, KI 318 bp.
(e) Schematic representation of the position of the genotyping primers in the various alleles.

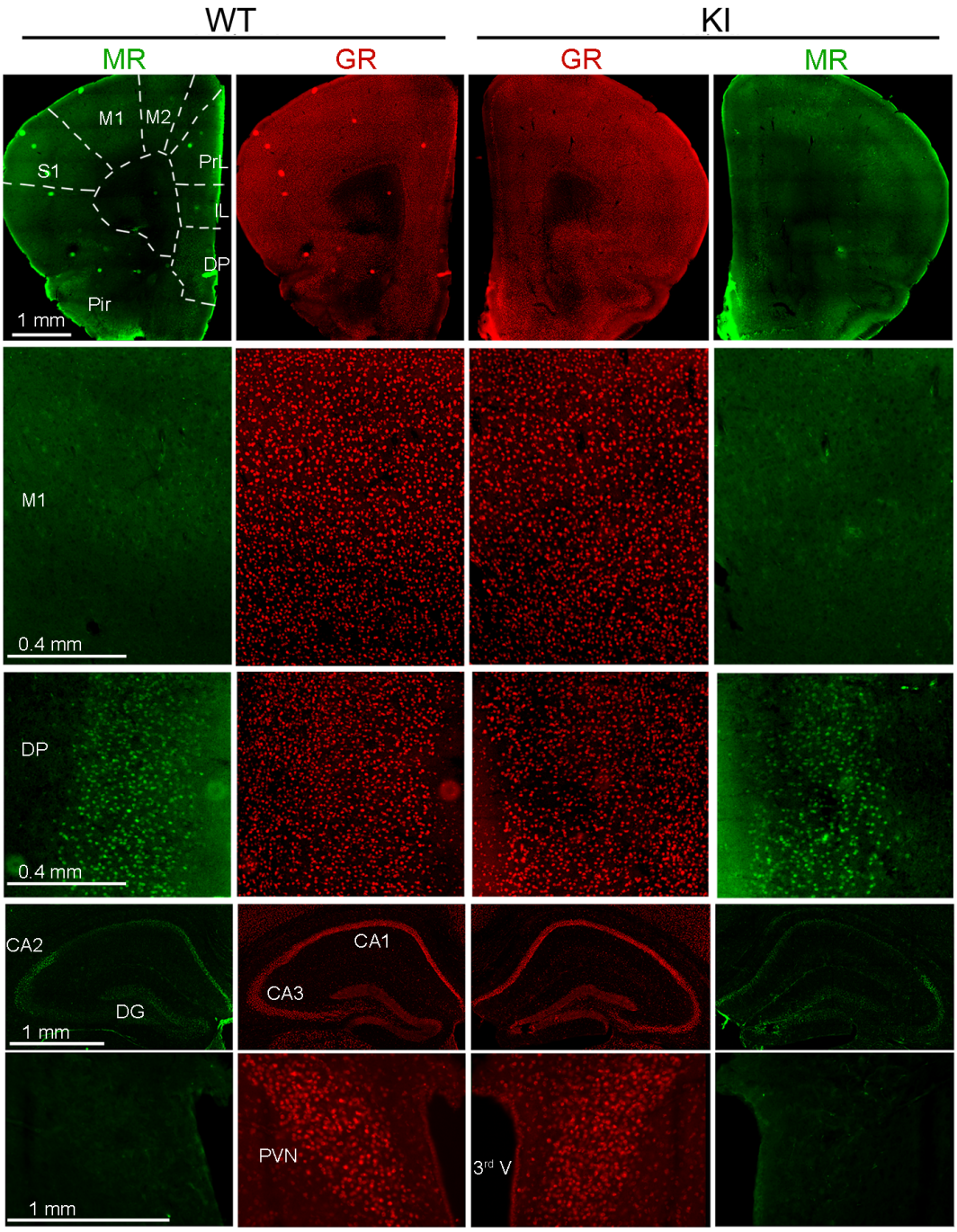

Figure S4. Expression of glucocorticoid receptors (GR and MR) in brain of KI mice. Detection of GR and MR in frontal cortex, hippocampus and hypothalamus reveals no difference of expression between WT and KI mice. M1-2 = motor area 1-2; S1 = sensory cortex area 1; Prl = prelimbic cortex; Il = infralimbic cortex; DP = dorsal peduncular cortex; Pir = piriform cortex; CA1-3 = cornus ammonis area 1-3; PVN = hypothalamic paraventricular nucleus.

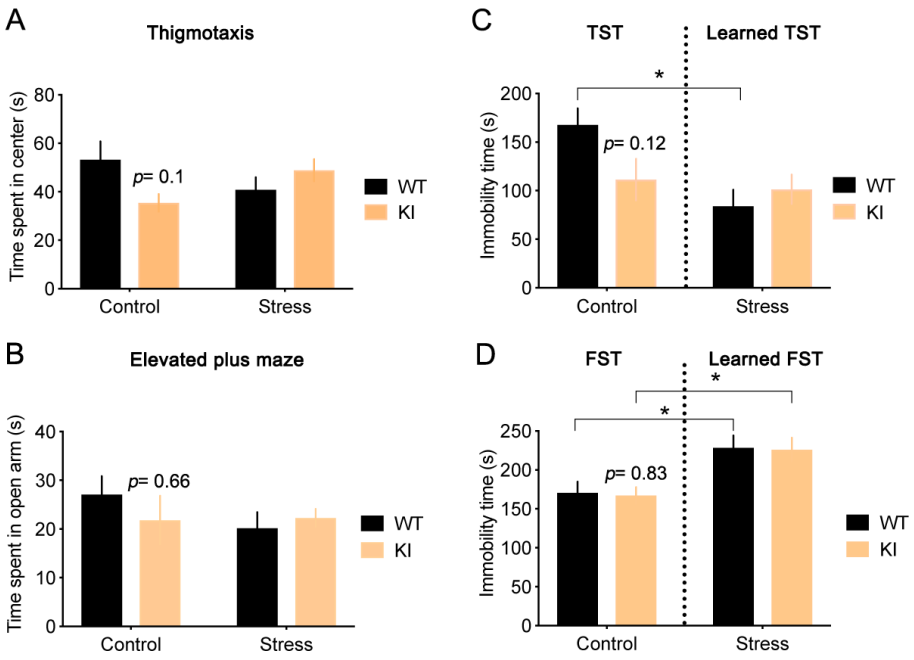

Figure S5. No significant effects of genotype on the expression of anxiety and despair-like behaviors at 3 month of age

(A) Time spent in the center arena of the open field. Means ±SEM of n=12 mice/ group, 2-way ANOVA: interaction of chronic unpredictable stress (for 3 weeks after weaning) and genotype $F_{1,44}$=5.7, p=0.0212 although genotype or stress alone had no effect.

(B) Time spent in the open arm of the elevated plus maze. No effect of chronic stress (for 3 weeks after weaning) and genotype alone or in interaction (means ±SEM of n=11 mice/ group).

(C) Time spent immobile in the tail suspension test (TST). Means ±SEM of n=11 mice/ group, 2-way ANOVA: Effect of habituation to the TST (Learned TST) in the stress group pre-exposed to this test once a week for 3 weeks $F_{1,40}$=6.9, p=0.0119.

(D) Time spent immobile in the forced swim test (FST). Means ±SEM of n=11 mice/ group, 2-way ANOVA: Effect of habituation to the FST (Learned FST) in the stress group pre-exposed to this test twice a week for 3 weeks $F_{1,40}$=16.94, p=0.0002.

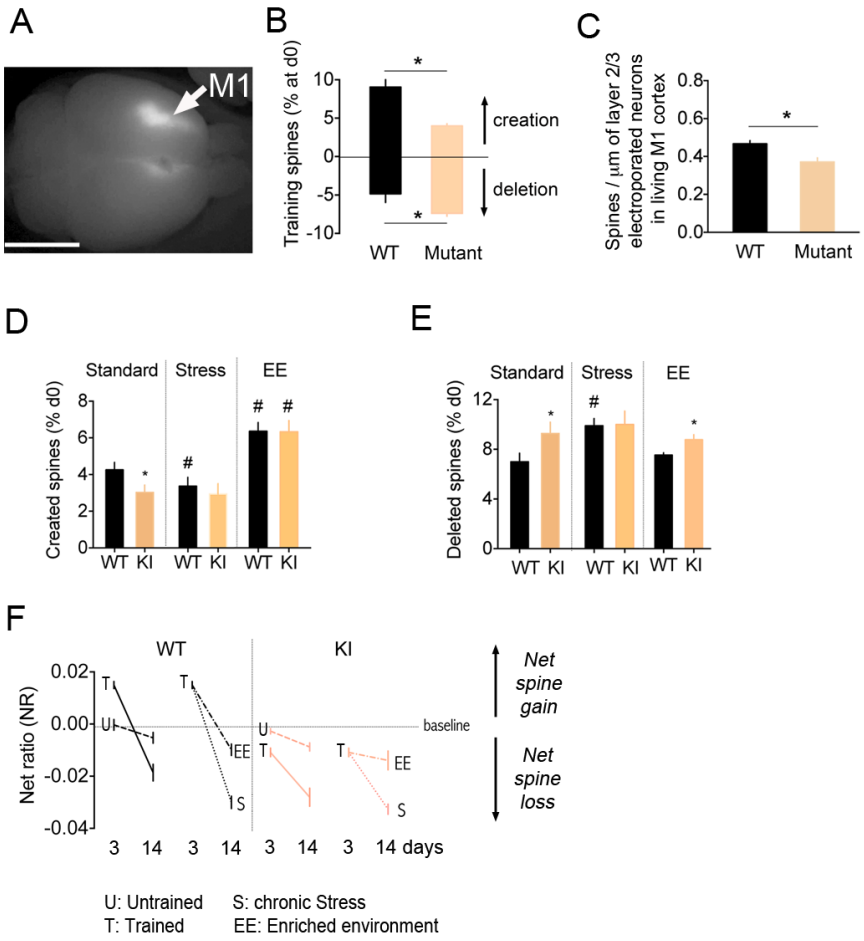

Figure S6. Effect of GR-PO$_4$ deletion on experience-dependent spine dynamics.
(A) *In utero* electroporation of GR constructs in excitatory NG neurons of M1 for substituting endogenous GR by recombinant GR-WT or mutant. Scale =4 mm.
(B) Remodeling of training spines in NG neurons electroporated with GR constructs. Means ±SEM of n=8 WT and 14 GR-mutant. Two-way ANOVA: Effect of GR-mutant $F_{(1,38)}$=25.1, p<0.0001, effect of spine remodeling $F_{(2,38)}$=225, p<0.0001, post-hoc Tukey test for spine creation *p=0.0008 and for spine deletion *p=0.031.
(C) Spine density at P35 in NG neurons of M1 electroporated with GR constructs. Means ±SEM of n=8 WT and 14 GR-mutant, unpaired t-test $t_{(11)}$=3.59 *p=0.0042.
(D) Spine formation (means ±SEM of n=8 WT standard, 8 KI standard, 7 WT stress, 7 KI stress and 7 WT EE, 7 KI EE mice). Two-way ANOVA: Effect of EE $F_{(1,26)}$=39.6, p<0.0001 post-hoc Tukey test in WT $^{\#}p$=0.027 and in KI $^{\#}p$<0.0001. Effect of chronic stress $F_{(1,26)}$=4.68, p=0.0039 post-hoc Tukey test $^{\#}p$=0.03.
(E) Spine deletion (means ±SEM of n=8 WT standard, 8 KI standard, 7 WT stress, 7 KI stress and 7 WT EE, 7 KI EE mice). Two-way ANOVA Effect of EE $F_{(1,26)}$=34.9, p<0.0001, post-hoc Tukey test in new spines *p=0.0002, in old spines *p=0.014. Effect of stress $F_{(1,26)}$=9.13, p=0.005 post-hoc Tukey test $^{\#}p$=0.0093.
(F) The fraction of spines gained subtracted of the spines lost day to day, were calculated as net ratio (NR) = (N_{formed} - $N_{deleted}$)/(2 × N_{total}). Means ± SEM of n=6 WT and 6 KI untrained, 21 WT and 18 KI trained, 7 WT and 6 KI stress, 7 WT and 6 KI EE. Two-way ANOVA: effect of

training in WT $F_{(1,36)}$=0.6 and in KI $F_{(1,32)}$=34.6, p<0.0001; effect of stress in WT $F_{(1,52)}$=9.7; p=0.0029 and in KI $F_{(1,44)}$=1; effect of EE in WT $F_{(1,52)}$=5.8; p=0.019 and in KI $F_{(1,44)}$=8.52; p=0.0055.

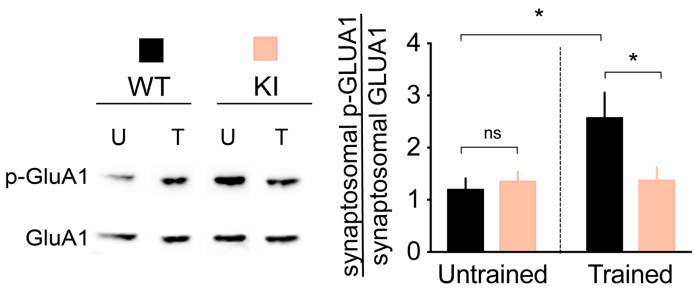

Figure S7. Effect of GR-PO$_4$ deletion on training-induced GluA1 phosphorylation in motor cortex.
(A) Synaptosomal GluA1-PO$_4$/GluA1 in M1 cortex. Means ±SEM, n=7 mice/group, 2-way ANOVA Effect of training $F_{1,24}$=5.7, p=0.025; training x genotype $F_{1,24}$=5.54, p=0.027 post-hoc Tukey test *p<0.05.

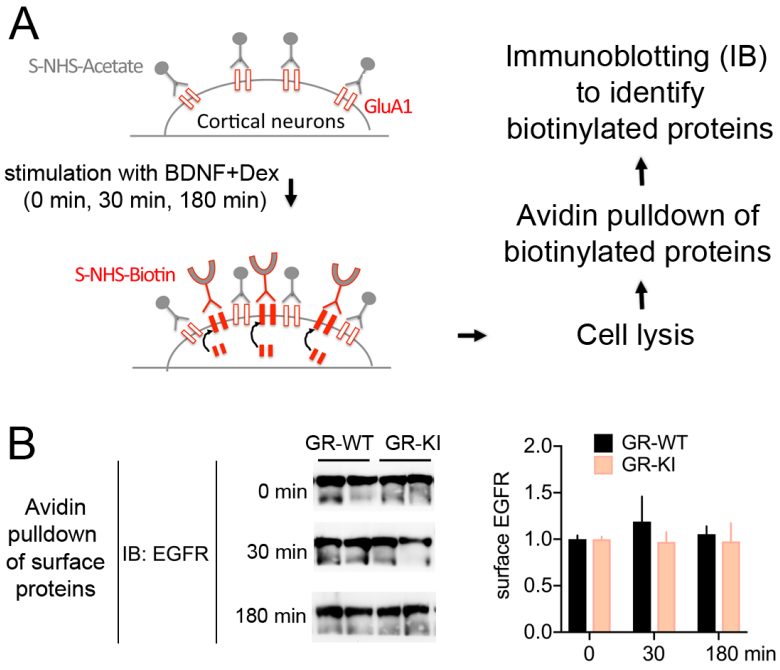

Figure S8. No effect of GR-PO$_4$ deletion on the cell surface expression of EGFR.
(A) Schematic representation of the procedure to isolate and monitor the dynamics of proteins insertion at the cell surface. Sulfo-NHS-acetate blocks all sites at the cell surface such that Sulfo-NHS-biotin can label newly inserted proteins. After cell lysis, avidin pulldown with magnetic beads allows for the purification of cell surface proteins that can be further identified by immunoblotting with specific antibodies.
(B) Avidin pulldown of biotinylated EGFR from neurons stimulated with 25 ng/ml BDNF and 1 μM Dex for the indicated time. Surface EGFR in cortical neurons expressing GR-WT or GR-KI constructs. Means ±SEM of n=5 WT and 5 KI/group, 2-way ANOVA: Effect of mutant $F_{1,24}$=0.67, p=0.4.

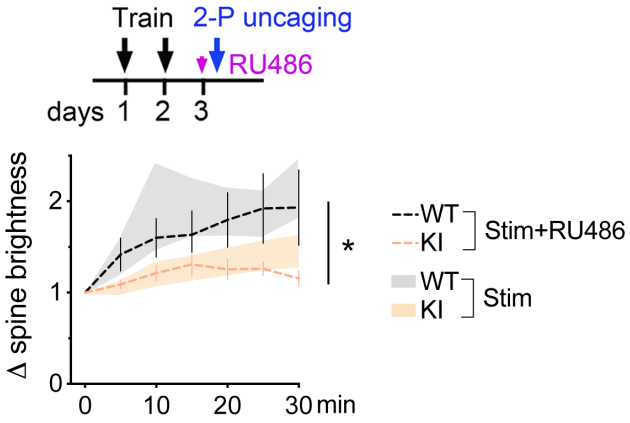

Figure S9. No acute effect of RU486 on glutamate-evoked spine enlargement in motor cortex.

Mice trained on the rotarod for 2 days were administered with RU486 (20 mg/kg, IP) 20 min before 2-P uncaging of glutamate at specific spine synapses in motor cortex. Means ±SEM of n=22 stim WT spines and 12 stim+RU486 WT spines, 40 stim KI spines and 18 stim+RU486 KI spines in 6 mice. Two-way ANOVA: Effect of RU486 $F_{3,593}$=11.57, p<0.0001; effect of time $F_{6,593}$=4.64, p=0.0001, post-hoc Tukey's test *p<0.0127.

Antibodies

Immunogen	Details	Source	Comments	Manufacturer
GR-PO_4	S152 –P (S155-P in rat)	Rabbit polyclonal Affinity purified	Use at 1.5 mg/ml, epitope unmasking in 10 mM Tris PH=9, 1 mM EDTA, 0,05% tween for 20 min	Homemade (Lambert et al., 2013)
GR-PO_4	S284-P (S287-P in rat)	Rabbit polyclonal Affinity purified	Use at 1.5 mg/ml, epitope unmasking in 10 mM Tris PH=9, 1 mM EDTA, 0,05% tween for 20 min	Homemade (Lambert et al., 2013)
GR-PO_4	S246-P	Rabbit polyclonal Whole serum	Use at 1:500-2000	Homemade (Ismaili and Garabedian, 2004)
GR-PO_4	S232-P	Rabbit polyclonal Whole serum	Use at 1:1000	Homemade (Ismaili and Garabedian, 2004)
GR-PO_4	S224-P	Rabbit polyclonal Whole serum	Use at 1:1000	Homemade (Ismaili and Garabedian, 2004)
GR	M20	Rabbit polyclonal	Use at 1:400	Santa Cruz Biotechnologies
Erk1/2		Rabbit polyclonal	Use at 1:1000	Santa Cruz Biotechnologies
Parvalbumin		Mouse polyclonal	Use at 1:3000	Swant
Neurogranin	Ab5620	Mouse polyclonal	Use at 1:5000, epitope unmasking in 10 mM Tris PH=9, 1 mM EDTA, 0,05% tween for 20 min	Millipore
GFP		Chicken polyclonal	Use at 1:2000	Abcam
RFP		Rabbit polyclonal	Use at 1:1000	Rockland
GR	BuGr2	Mouse monoclonal	Use at 1:1000	Calbiochem
PSD95	clone K28/43	Mouse monoclonal	Use at 1:1000	NeuroMab
Synaptophysin		Rabbit monoclonal	Use at 1:1000	Life Technologies
EGFR		Rabbit polyclonal	Use at 1:1000	Cell Signaling Techologies
GLUA1		Rabbit polyclonal	Use at 1:1000	Millipore
GLUA1-PO_4		Rabbit monoclonal	Use at 1:1000	Millipore
c-FOS		Mouse monoclonal	Use at 1:100, epitope unmasking in 10 mM Tris PH=9, 1 mM EDTA, 0,05% tween for 20 min	Santa Cruz Biotechnologies
c-FOS	#2250	Rabbit monoclonal	Use at 1:1000	Cell Signaling
AlexA Fluor conjugated secondary antibodies		Rabbit monoclonal	Use at 1:2000	ThermoFisher Scientific

Drugs

Compound name	Effect	Working concentration	comments	Manufacturer
PMSF	Protease inhibitor	100 ng/ml	In lysis buffer	Sigma
Aprotinin	Protease inhibitor	100 nM	In lysis buffer	Sigma
Leupeptin	Protease inhibitor	100 nM	In lysis buffer	Sigma
Na_3VO_4	Tyr Phosphatase inhibitor	1 mM	In lysis buffer	Sigma
NaF	Phosphatase inhibitor	100 nM	In lysis buffer	Sigma
calyculin A	Phosphatase inhibitor	10 nM	In lysis buffer	Sigma
BDNF	Neurotrophin	25 ng/ml	TrkB agonist	Sigma
Dexamethasone	Synthetic glucocorticoid	1 µM in vitro	GR agonist	Sigma
Bicuculline methiodide	GABAA receptor antagonist	3.5 mM	Touch application	Sigma
MNI-glutamate	Caged-ligand Photoactivable	20 mM	Topical application	Sigma
RU486	GR antagonist	20 mg/kg	intraperitoneal	Sigma
sulfo-NHS-acetate	Block cell surface proteins	1.5 mg/ml	Use in TBS, 30 min at 4°C	Pierce
sulfo-NHS-LC-biotin	Labeling of surface proteins	0.5 mg/ml	Use in TBS, 30 min at 4°C	Pierce
Glycine	Quench reactive sulfo-NHS moieties	100 mM	Use in PBS, 20 min at 4°C	Sigma
Uridine		10 mM	Use with 5FU	Sigma
5-fluoro-uridine		10 mM	Block cell proliferation	Sigma
B27	Serum free	2% (v/v)	Culture supplement	Life Technologies

Primers	
Gene	**For genotyping of GR knockin mouse**
Primer_01F	5'-GCAGGCCGCTCAAGTGTTTTCT-3'
primer_02R	5'-CACTGACCAACGAGAAACGATTAC-3'
primer_03F	5'-GCAGGCAGAAGTGTGTTTAGC-3'
primer_04R	5'-CAGTCATAGCCGAATAGCCTCTC-3'
primer_05F	5'-CTGAGGGTGAAGACGCAGAAAC-3'

Table S1. List of antibodies, primers and chemical reagents used in study.